# Large-Scale Functional Assessment of Genes Involved in Rare Diseases with Intellectual Disabilities Unravels Unique Developmental and Behaviour Profiles in Mouse Models

Hamid Meziane, Marie-Christine Birling, Olivia Wendling, Sophie Leblanc, Aline Dubos, Mohammed Selloum, Guillaume Pavlovic, Tania Sorg, Vera M. Kalscheuer, Pierre Billuart, et al.

biomedicines

MDPI

*Article*

# Large-Scale Functional Assessment of Genes Involved in Rare Diseases with Intellectual Disabilities Unravels Unique Developmental and Behaviour Profiles in Mouse Models

**Hamid Meziane [1], Marie-Christine Birling [1], Olivia Wendling [1], Sophie Leblanc [1], Aline Dubos [1,2], Mohammed Selloum [1], Guillaume Pavlovic [1], Tania Sorg [1], Vera M. Kalscheuer [3], Pierre Billuart [4,5], Frédéric Laumonnier [6,7], Jamel Chelly [2], Hans van Bokhoven [8,9,10] and Yann Herault [1,2,*]**

1 Université de Strasbourg, CNRS, INSERM, Institut Clinique de la Souris (ICS), PHENOMIN, CELPHEDIA, 1 rue Laurent Fries, 67404 Illkirch, France
2 Université de Strasbourg, CNRS, INSERM, Institut de Génétique et de Biologie Moléculaire et Cellulaire, 1 rue Laurent Fries, 67404 Illkirch, France
3 Max Planck Institute for Molecular Genetics, Research Group Development and Disease, Ihnestr. 63-73, 14195 Berlin, Germany
4 Institute of Psychiatry and Neuroscience of Paris (IPNP), Université de Paris, INSERM U1266, "Genetic and Development of Cerebral Cortex", 75014 Paris, France
5 GHU Paris Psychiatrie et Neurosciences, Hôpital Sainte Anne, 75014 Paris, France
6 UMR 1253, iBrain, University of Tours, Inserm, 37032 Tours, France
7 Service de Génétique, Centre Hospitalier Régional Universitaire, 37044 Tours, France
8 Department of Cognitive Neuroscience, Radboudumc, 6500 HB Nijmegen, The Netherlands
9 Department of Human Genetics, Radboudumc, 6500 HB Nijmegen, The Netherlands
10 Donders Institute for Brain, Cognition, and Behaviour, Centre for Neuroscience, 6525 AJ Nijmegen, The Netherlands
* Correspondence: herault@igbmc.fr; Tel.: +33-388-65-5715

**Abstract:** Major progress has been made over the last decade in identifying novel genes involved in neurodevelopmental disorders, although the task of elucidating their corresponding molecular and pathophysiological mechanisms, which are an essential prerequisite for developing therapies, has fallen far behind. We selected 45 genes for intellectual disabilities to generate and characterize mouse models. Thirty-nine of them were based on the frequency of pathogenic variants in patients and literature reports, with several corresponding to de novo variants, and six other candidate genes. We used an extensive screen covering the development and adult stages, focusing specifically on behaviour and cognition to assess a wide range of functions and their pathologies, ranging from basic neurological reflexes to cognitive abilities. A heatmap of behaviour phenotypes was established, together with the results of selected mutants. Overall, three main classes of mutant lines were identified based on activity phenotypes, with which other motor or cognitive deficits were associated. These data showed the heterogeneity of phenotypes between mutation types, recapitulating several human features, and emphasizing the importance of such systematic approaches for both deciphering genetic etiological causes of ID and autism spectrum disorders, and for building appropriate therapeutic strategies.

**Keywords:** mouse model; genetic modification; intellectual disability; behavior phenotypes

check for updates

**Citation:** Meziane, H.; Birling, M.-C.; Wendling, O.; Leblanc, S.; Dubos, A.; Selloum, M.; Pavlovic, G.; Sorg, T.; Kalscheuer, V.M.; Billuart, P.; et al. Large-Scale Functional Assessment of Genes Involved in Rare Diseases with Intellectual Disabilities Unravels Unique Developmental and Behaviour Profiles in Mouse Models. *Biomedicines* **2022**, *10*, 3148. https://doi.org/10.3390/biomedicines10123148

Academic Editors: Madelyn A. Gillentine

Received: 23 October 2022
Accepted: 2 December 2022
Published: 6 December 2022



## 1. Introduction

Intellectual disability (ID) is a major medical and socio-economic problem owing to its high incidence in the general population. Mutations in about 1500 different genes have been associated with ID [1,2], while pathogenic mechanisms and the molecular basis of gene dysfunction in ID remains to be elucidated. So far, functional studies have mainly focused on single gene defects, such as the Fragile X syndrome. Here, we propose a systematic

approach to gain pathway-based insights into mechanisms leading to cognitive dysfunction in humans.

Based on human genetic studies, we selected 45 genes (Table 1) to generate and characterize mutant mice models, of which 39 were selected based on the frequency of pathogenic variants in ID patients. The proteins encoded by these genes act in various biological processes, such as transcription regulation, epigenetic modification, synaptic transmission, or influencing the excitatory/inhibitory balance of central nervous system (CNS) activity. In patients with ID, 31 genes of this selection carry loss-of-function (LoF) variants or deletions, with two genes displaying additional gain-of-function (Gof) mutations, two genes carrying splicing variants, and 12 genes carrying missense variants. Most of these pathogenic variants cause a syndromic ID disorder. Six other genes potentially involved in ID were included, namely *ASCC3* found mutated in a single family by performing a large-scale genomic study [3], *EHMT2* homologous to *EHMT1* causing Kleefstra syndrome, and *CDK8. CDK8* encodes a key subunit of the Mediator complex involved in transcriptional processes and harbouring pathogenic variants in several other subunits, causing syndromic or non-syndromic ID. Two additionally included genes were found mutated in single patients with ID (*CDC27, mIR124a-2*). We also added *STARD8*, which is deleted or disrupted in patients with a contiguous gene deletion and craniofrontonasal syndrome [4,5], and encodes a Rho GTPase-activating protein, like *OPHN1* whose LoF causes X-linked ID [6]. Thirty of the selected genes are located on an autosome and 15 on the X chromosome. Thus, we generated, characterized and compared male mouse models carrying either a mutation identical to a patient with ID or a LoF allele to better understand the function of a candidate ID gene.

**Table 1.** List of mutated genes, human variants, their functional implication in human syndromes, and mouse models generated in this study for these genes. LoF and GoF indicate loss-of-function and gain-of-function, respectively. SNPs indicate Single Nucleotide Polymorphism.

| *Gene* | Chr | Human Variant(s) | Syndrome(s) | References | Mouse Models |
|---|---|---|---|---|---|
| *Ankrd11* | 8 | LoF mutations and deletion (heterozygous) | KBG Syndrome | [7] | $Ankrd11^{Camk2a}$ |
| *Arx* | X | LoF mutations, deletion, duplication/expansion (hemizygous) 24bp duplication most frequent mutation | Early infantile epileptic encephalopathy 1, Hydranencephaly with abnormal genitalia, X-linked lissencephaly 2, X-linked Mental retardation, Partington syndrome, Proud syndrome | [8–10] | $Arx^{Dup24/y}$ |
| *Ascc3* | 10 | - | - | - | $Ascc3^{Camk2a}$ |
| *Atp6ap2* | X | Splice site and missense (hemizygous) | ID +/− Parkinsonism with spasticity | [11,12] | $Atp6ap2^{Camk2a/y}$ |
| *Cdc27* | 11 | - | - | - | $Cdc27^{-/-}$; $Cdc27^{S92F}$ |
| *Cdk8* | 5 | Missense substitutions | - | [13] | $Cdk8^{-/-}$; $Cdk8^{Camk2a/y}$ |
| *Cdkl5* | X | Translocations, microdeletions, missense, LoF mutations & mosaic exonic deletions (hemizygous in males & heterozygous in females) | CDKL5 Deficiency disorder (CDD) & Early Infantile Epileptic Encephalopathy 2 (EIEE2) | [14,15] | $Cdkl5^{-/y}$ |
| *Cntnap2* | 6 | LoF mutations & SNPs (homozygous or compound heterozygous) | Cortical Dysplasia-Focal Epilepsy Syndrome (CDFES), Pitt-Hopkins like syndrome 1 & Autism & Specific Language Impairment | [16–18] | $Cntnap2^{-/-}$ |
| *Dnmt3b* | 2 | LoF mutations (homozygous or compound heterozygous) | Immunodeficiency-centromeric instability-facial anomalies syndrome 1 | [19,20] | $Dnmt3b^{D803G/-}$ |
| *Dync1h1* | 12 | LoF mutations (heterozygous) | Autosomal dominant axonal Charcot-Marie-Tooth type 20 disease (CMT20), Autosomal dominant mental retardation 13 (MRD13), Autosomal dominant lower extremity-predominant Spinal muscular atrophy 1 (SMALED1) | [21–23] | $Dync1h1^{-/-}$; $Dync1h1^{K3334N}$ |
| *Dyrk1a* | 16 | Translocations, LoF mutations & deletions (heterozygous) | Autosomal Dominant Mental Retardation 7 (MRD7) | [24] | $Dyrk1a^{-/-}$; $Dyrk1a^{Camk2a}$; $Dyrk1a^{Dlx5-6/+}$ |
| *Ehmt1* | 2 | Translocations, microdeletion & LoF mutations (heterozygous) | Kleefstra syndrome | [25,26] | $Ehmt1^{+/-}$ |
| *Ehmt2* | 17 | - | - | - | $Ehmt2^{+/-}$ |
| *Entpd1* | 19 | LoF mutations (homozygous) | Autosomal Recessive Spastic Paraplegia 64 (SPG64) | [27] | $Entpd1^{-/-}$ |

**Table 1.** *Cont.*

| *Gene* | Chr | Human Variant(s) | Syndrome(s) | References | Mouse Models |
|---|---|---|---|---|---|
| *Frmpd4* | X | LoF mutations, missense and exon deletion (hemizygous) | X-linked Intellectual disability & Schizophrenia | [28,29] | *Frmpd4*$^{-/y}$ |
| *Gatad2b* | 3 | LoF mutations & deletions (heterozygous) | Intellectual disability | [30] | *Gatad2b*$^{-/-}$ |
| *Il1rap1l1* | X | LoF mutations (hemizygous) | X-linked intellectual disability | [31,32] | *Il1rpl1*$^{-/y}$ |
| *Kansl1* | 11 | LoF mutations & deletions (heterozygous) | Koolen-De Vries syndrome | [33] | *Kansl1*$^{-/-}$ |
| *Kdm5c* | X | LoF mutations (hemizygous) | Claes-Jensen type X-linked syndromic mental retardation | [34] | *Kdm5c*$^{-/y}$; *Kdm5c*$^{Camk2a/y}$; *Kdm5c*$^{Dlx5-6/y}$ |
| *Kif5c* | 2 | LoF mutations (heterozygous) | Complex Cortical Dysplasia with Other Brain Malformations 2 (CDCBM2) | [22] | *Kif5c*$^{+/-}$; *Kif5c*$^{E237V}$ |
| *Klhl15* | X | LoF mutations & deletions (hemizygous) | Intellectual disability | [28] | *Klhl15*$^{-/y}$ |
| *Larp7* | 3 | LoF mutations & duplications (homozygous) | Alazami syndrome | [3,35] | *Larp7*$^{-/y}$ |
| *Mbd5* | 2 | LoF mutations, translocation, duplications & deletions (heterozygous) | Autosomal Dominant Mental Retardation 1 (MRD1) & 2q23.1 duplication and deletion syndromes | [36–38] | *Mbd5*$^{-/-}$ |
| *Mecp2* | X | LoF mutations (heterozygous in females) | Rett syndrome, Atypical Rett Syndrome or Angelman-like Phenotype & Autism | [39,40] | *Mecp2*$^{-/y}$ |
| *Med12* | X | Missense mutations (hemizygous) p.(R961W) most frequent mutation | Lujan-Fryns syndrome, X-linked Ohdo syndrome & Opitz-Kaveggia syndrome | [41–43] | *Med12*$^{-/y}$; *Med12*$^{R961X}$ |
| *Med17* | 9 | p.(L371P) missense mutation (homozygous) | Postnatal progressive microcephaly with seizures and brain atrophy | [44] | *Med17*$^{L369P}$ |
| *Med23* | 10 | p.(R617Q) missense mutation (homozygous) | Autosmal recessive intellectual disability 18 | [45] | *Med23*$^{-/-}$; *Med23*$^{R617Q}$ |
| *Med25* | 7 | Missense mutations (homozygous) | Autosmal recessive Charcot-Marie-Tooth type 2B2 disease & Basel-Vanagait-Smirin-Yosef syndrome (BVSYS) | [46,47] | *Med25*$^{-/-}$ |
| *mIR124a-2* | 3 | - | - | - | *Mir124*$^{-/-}$ |
| *mIR137* | 3 | Microdeletions (heterozygous) | Intellectual disability, autism & schizophrenia | [48,49] | *Mir137*$^{-/-}$ |
| *Nr1i3* | 1 | LoF mutations (heterozygous) | Core features of Kleefstra syndrome | [50] | *Nr1i3*$^{-/-}$ |
| *Pafah1b1* | 11 | LoF mutations, deletion & translocation (heterozygous) | Lissencephaly 1, Miller-Dieker lissencephaly syndrome & Subcortical laminar heterotopia | [51,52] | *Pafah1b1*$^{-/-}$ |
| *Phf6* | X | LoF Mutations (heterozygous in females & hemizygous in males) | Borjeson-Forssman-Lehmann syndrome (BFLS) | [53] | *Phf6*$^{-/y}$ |
| *Phf8* | X | LoF mutations & deletion (hemizygous) | Siderius X-linked Mental retardation syndrome (MRXSSD) | [54] | *Phf8*$^{-/y}$ |
| *Prps1* | X | LoF & GoF mutations (hemizygous) | LoF: Arts syndrome, X-linked recessive Charcot-Marie-Tooth disease 5 & X-linked non syndromic hearing loss (NSHL) vs. GoF: PRPS-related Gout syndrome & Phosphoribosylpyrophosphate Synthetase Superactivity | [55–57] | *Prps1*$^{-/y}$; *Prps1*$^{Camk2a/y}$; *Prps1*$^{Csps4/y}$ |
| *Ptchd1* | X | LoF mutations & deletion (hemizygous) | X-linked Autism Susceptibility (AUTSX4) | [58,59] | *Ptchd1*$^{-/y}$ |
| *Scaper* | 9 | LoF mutation (homozygous & compound heterozgous) | Retinitis pigmentosa with intellectual disability | [60] | *Scaper*$^{-/-}$ |
| *Setbp1* | 18 | GoF mutations (Schinzel-Giedion Syndrome) & LoF mutations (autosmal dominant mental retardation 29) (heterozygous) | Schinzel-Giedion Syndrome vs. Autosomal dominant Mental Retardation syndrome 29 (MRD29) | [61–63] | *Setbp1*$^{-/-}$ |
| *Stard8* | X | - | - | - | *Stard8*$^{-/y}$ |
| *Taf2* | 15 | Missense mutations (homozygous) | Autosomal recessive Mental retardation 40 (MRT40) | [3,64] | *Taf2*$^{-/-}$ |
| *Tti2/C8orf41* | 8 | Missense mutations (homozygous) | Autosomal recessive Mental retardation 39 (MRT39) | [3,65] | *Tti2*$^{-/-}$ |
| *Tubb3* | 8 | LoF mutations (heterozygous) | Complex Cortical Dysplasia with Other Brain Malformations (CDCBM1) & Congenital Fibrosis of Extraocular Muscles 3a (CFEOM3A) | [66,67] | *Tubb3*$^{M388V}$ |
| *Tubg1* | 11 | Missense mutations (heterozygous) | Complex Cortical dysplasia with other brain malformations 4 (CDCBM4) | [22] | *Tubg1*$^{-/-}$; *Tubg1*$^{Y92C}$ |
| *Wdr62* | 7 | LoF mutations (homozygous) | Autosomal recessive primary Microcephaly 2 with or without cortical malformations | [68,69] | *Wdr62*$^{-/-}$ |
| *Zc4h2* | X | Missense & in frame insertion (hemizygous in males), LoF mutations, splice site, missense & (partial) gene deletions (heterozygous in females) | ZC4H2-Associated Rare Disorders (ZARD), previously known as Wieacker-Wolff syndrome (WRWF) | [70,71] | *Zc4h2*$^{-/y}$ |

Different types of strategies were followed for generating the appropriate models (see Section 2 and Figure S1). Subsequently, we assessed the viability of the mutant mouse lines. Twenty-seven lines were further investigated using a standardized behavioural screen, focusing on males since a wide range of disorders associated with ID are X-linked ID and 33% of genes in the present study are located on the X-chromosome. Several tests were used to assess a wide range of functions or their pathologies, including circadian activity, neurological reflexes and specific motor abilities, anxiety-related behaviour, sensorimotor gating, and learning and memory processes. For some mouse lines, additional tests were performed to further characterize abnormalities observed or to extend phenotypic traits related to individual genes.

## 2. Materials and Methods

The procedures carried out in this project were performed in agreement with the EC directive 2010/63/UE86/609/CEE, submitted to the French Ethics Committee 017 (Com'Eth) and received accreditation under number 2012-139.

### *2.1. Generation of ID Mouse Models*

Different strategies were used to obtain the appropriate mouse lines for genes involved in ID (Figure S1: Mouse models generated and phenotyped in the Gencodys consortium). Four mouse lines were repatriated to serve as reference lines and to extend phenotyping data reported in the literature (*Ehmt1*$^{tm1Yshk}$ [72,73], *Il1rapl1*$^{tm1.1Hesk}$ [74], *Mecp2*$^{tm1Hzo}$ [75]) or to study a candidate ID gene (*Ehmt2*$^{Gt(ES62)Feil}$ [76,77]). Forty-six mouse lines were generated as part of the European Conditional Mouse Mutagenesis Program (EUCOMM, 13 lines), Knock-Out Mouse Project (KOMP, 2 lines), the Mouse Genome Project at the WTSI (1 line) or directly in this effort (30 lines); they were all linked to the International Mouse Phenotyping Consortium (IMPC, mousephenotype.org). Mutations were either full knock-out (KO) or KO with conditional potential (40 lines), point mutations (PM, 9 lines) for *Cdc27(S92F), Dnmt3b(D803G), Dync1h1(K3334N), Kif5c(E237V), Med12(R961W), Med17(L369P), Med23(R617Q), Tubb3(M388V), Tubg1(Y92C)*, or humanisation, leading to a duplication of a poly-alanine stretch for *Arx* [10]. All mouse lines were either generated in a C57BL/6N genetic background or backcrossed on the C57BL/6N background. Some mutations induced lethality at the heterozygous or homozygous stage (Figure 1A; Figure S1: mouse models generated and phenotyped in the Gencodys consortium). Therefore, conditional mutants were generated for a selection of genes to overcome this problem, and different alleles were customized to study the potential contribution of specific neuronal (glutamatergic, GABAergic) or non-neuronal (glial) cellular networks using transgenic lines expressing Cre under the control of the *Camk*2a [78], *Dlx5-6* [79] or *Cspg4* [80] promoter.

### *2.2. Embryonic Pipeline*

The viability/sub-viability of mutants was assessed by crossing heterozygous mice and scoring the offspring's genotypic distribution. Selected lines with homozygous/hemizygous (or heterozygotes) scores below the Mendelian ratio were analysed using the well-defined embryo pipeline that we developed in the IMPC [81]. Briefly, embryos were collected at specific developmental stages to determine their window of lethality (Figure 1B) and further characterize their developmental defects.

### *2.3. Behavioural Phenotyping Strategy*

For each mutant line, cohorts of wildtype (WT) and mutant male mice were generated for phenotyping (8–12 mice per genotype). Mice were group-housed (2–4 per cage) and allowed 1–2 weeks acclimation in the phenotyping area with controlled temperature (21–22 °C) under a 12-12 light-dark cycle (light on at 07 a.m.), with food and water available ad libitum. Behavioural testing was performed in 10 to 13-week-old adults and carried out in agreement with EC directive 2010/63/UE86/609/CEE, and under the ethics committee accreditation number 2012-139.

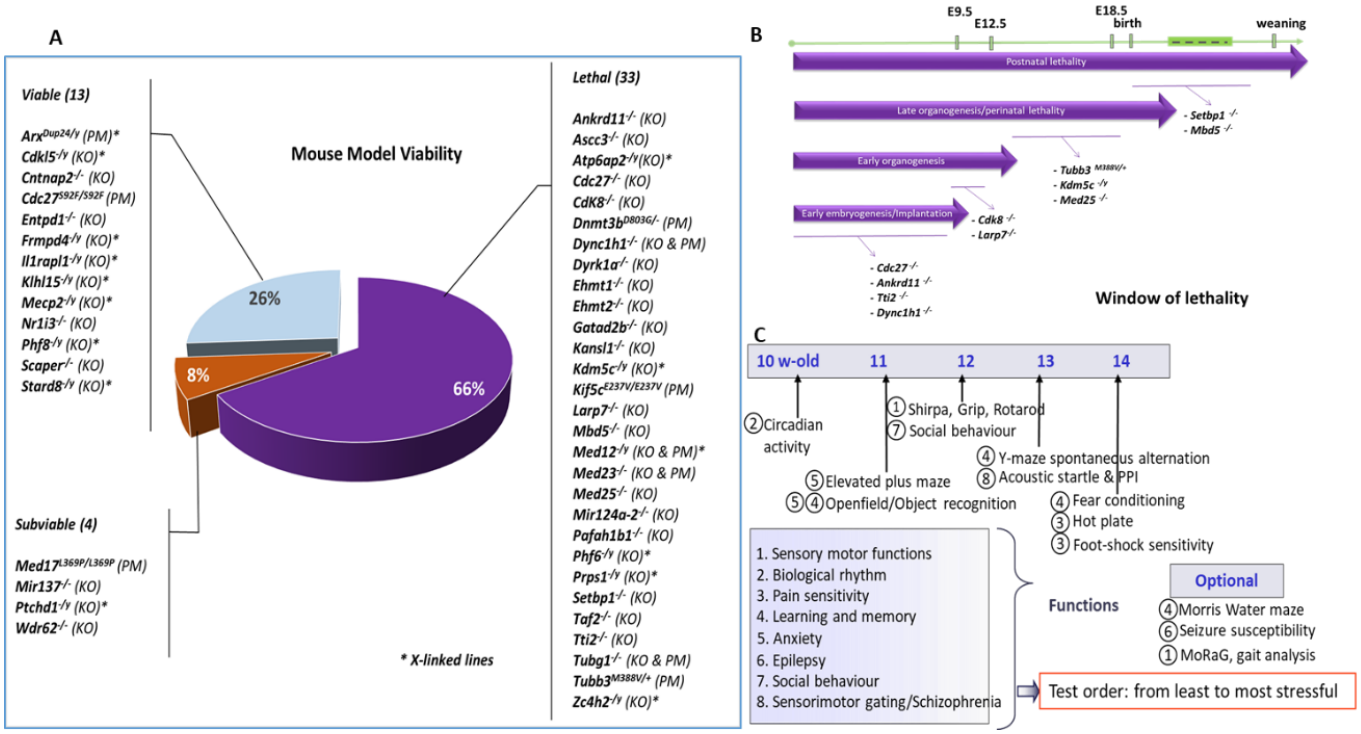


**Figure 1.** (**A**) Schematic representation of lethality. The percentage of lethal, sub-viable and viable mutant lines is presented with the list of lines for each category. (**B**) Time window of lethality analysed for 11 selected lethal lines. (**C**) Behavioural phenotyping scheme. Several tests were used for assessing a wide range of CNS functions; tests are ordered from least to most stressful.

Animals underwent a standardized behavioural screen composed of tests to assess sensory and motor abilities, biological rhythm, pain sensitivity, anxiety-related behaviour, sensorimotor gating, learning and memory, social behaviour, and susceptibility to seizures according to the ARRIVES guidelines [82]. Behavioural protocols are described in the Supplementary Materials; most of them are thoroughly detailed in a recent volume of current protocols [83]. The order of tests was carefully defined from the least to the most stressful test to reduce the potential influence of repeated testing (Figure 1C).

### *2.4. Statistical Analysis*

For each mutant line, phenotyping data were analysed using unpaired Student *t*-tests or repeated measures analyses of variance (ANOVA) with one between factor (genotype) and one within factor (time, etc.). Qualitative parameters (e.g., clinical observations) were analysed using the $\chi 2$ test. The level of significance was set at $p < 0.05$. A gene/phenotype heat-map was drawn based on *p*-values for each parameter (Table S1: Gene/phenotype heatmap).

In addition, other analyses were performed on all mutant lines related to categorized biological functions identified using appropriate parameters selected from the different behavioural tests. Fifty-seven (57) parameters were distributed in 10 categories representing biological functions (Table S2: categories of biological functions and related parameters). For each mutant line, a phenotype score (corresponding to the ratio of number of parameters having a phenotype) was calculated per biological function (Table S3: the phenotype scores). We considered that a parameter presents a phenotype if its adjusted *p*-value (using Benjamini-Hochberg method to control the false discovery rate within each biological function) was less than 0.05 (Supplementary Materials). Based on these phenotypic scores, Principal Component Analysis (PCA) was performed and a heatmap with cluster representation drawn (see the Section 3).

## 3. Results

### *3.1. Gene/Phenotype Relationship*

Fifty mutant lines were generated for 45 genes (Table 1 for genes and abbreviations). The viability of homozygous/hemizygous mutant mice was assessed by crossing the heterozygous mice. From the 50 mutant lines analysed, 66% displayed a homozygous/hemizygous lethality, 8% were sub-viable with less than the expected Mendelian progeny ratio [81], and 26% were viable (Figure 1A). Concerning the lines carrying a point mutation, seven out of nine presented homozygous lethality, and haploinsufficiency or autosomal dominant lethality was also found for *Med12* and *Tubb3*. Finally, of 16 lines with mutated genes on the X-chromosome (all alleles), seven were hemizygous lethal, eight viable and one showed sub-viability (Figure 1A).

This high rate of lethality/sub-viability could be expected, as these genes were selected based on their specific involvement in neurodevelopmental disorders. Indeed, the overall rate of homozygous lethality assessed in IMPC is approximately one out of three mutant genes [81] but increases dramatically when disease-related or essential genes are mutated [84].

To establish the time window of lethality and further characterize these essential genes, 11 mutant mouse lines were assessed (Figure 1B). Two of these lines displayed postnatal lethality (*Setbp1*$^{-/-}$, *Mbd5*$^{-/-}$), dying between birth and eight weeks, three lines displayed perinatal lethality and died during the viability test at E18.5 (*Tubb3*$^{M388V/+}$, *Kdm5c*$^{-/y}$, *Med25*$^{-/-}$), two lines died between E9.5 and E12.5 (*Cdk8*$^{-/-}$, *Larp7*$^{-/y}$), while four lines were lethal before E9.5 (*Cdc27*$^{-/-}$, *Ankrd11*$^{-/-}$, *Tti2*$^{-/-}$, *Dync1h1*$^{-/-}$). Three of the 11 selected lines were subjected to embryonic phenotyping (*Setbp1*$^{-/-}$, *Med25*$^{-/-}$ and *Tubb3*$^{M388V/+}$), revealing several morphological abnormalities early during development. *Setbp1*$^{-/-}$ mutants reacted to forceps stimuli and breathed normally at E18.5. High Resolution Episcopic Microscopy (HREM) and 3D reconstruction data at E15.5 revealed that *Setbp1*$^{-/-}$ mice displayed palatal (Figure S2: cranial and cervical vertebra abnormalities of *Setbp1*$^{-/-}$ mice at E15.5 and E18.5, panels B, C) and vertebral skeletal defects (Figure S2, panel I), reduced or absent dorsal root ganglia (DRG) (Figure S2, panels E, I) and abnormal nasopharyngeal opening (Figure S2, panel B). Vertebral fusion was confirmed at E18.5 by skeletal staining with red alizarin and alcian blue (Figure S2, panel G). *Tubb3*$^{M388V/+}$ mice at E18.5 were smaller than their WT counterparts (Figure S3: cranial nerve and associated ganglia as well as dorsal root ganglia abnormalities in *Tubb3*$^{M388V/M388V}$ mutant embryos, panel B), displayed weak or no reaction to forceps stimuli and died between 10 min and 30 min after delivery. HREM data at E15.5 revealed severe reduction of DRG and sensitive nerves in *Tubb3*$^{M388V/+}$ mutants (Figure S3, panels E, F), while motor fibres were still present. At the level of cranial nerves, *Tubb3*$^{M388V/+}$ mutants displayed agenesis of the trigeminal ganglion (Figure S3, panels H, J), hypoplasia of trigeminal nerves, facioacoustic ganglion and nerves, facial ganglion and nerves, glossopharyngeal and vagus nerves and hypoglossal nerves (Figure S3, panels I–K). Gross morphological analysis of *Med25*$^{-/-}$ mutants at E12.5 and E15.5 revealed different ranges of abnormalities including anophthalmia (Figure S4: severe craniofacial abnormalities in *Med25*$^{-/-}$ mutant embryos and foetuses, panel B), hypoplasia of the telencephalon (three out of twelve mice) (Figure S4, panel D), rhinocephaly with cyclopia (one out of twelve mice) (Figure S4, panels K, H), proboscis (one out of twelve mice) (Figure S4, panel G), facial clefts (two out of twelve mice) (Figure S4, panel E) and exencephaly (three out of twelve mice) (Figure S4, panels G, J).

Among the sub-viable mutant lines, *Med17*$^{-/-}$ showed decreased body weight, breathing difficulties, and died between P0 and eight weeks after birth. Necropsy examination revealed abdominal and pulmonary haemorrhage, hypoplasia of the thymus and heart failure.

These data strongly support the fact that around 65% of genes involved in ID are essential for survival at normal Mendelian ratios. To better understand the specific involvement of these genes in CNS functions, we generated brain specific conditional mutants.

Assessing the viability of mutant lines with a tissue specific *Camk2a* reporter revealed that five out of six lines were viable and one out of six lines was sub-viable.

We pursued the analysis with the standardized behavioural phenotyping of 27 mutant lines to detect a wide range of phenotypic traits affecting different CNS functions. As eight mutant lines were generated for X-linked genes with features found only in males, we focused the adult study on male mutant mice. The first observation of the gene/phenotype heatmap revealed three main classes of mutants based on activity phenotypes observed in the different behavioural tests (Table S1). The first group of mutated genes inducing a substantial increase in spontaneous activity, the second group of mutant lines with decreased spontaneous activity, and the third group of mutant lines with no change.

#### 3.1.1. Hyperactivity Group

The hyperactivity group includes $Cdk8^{Camk2a/Camk2a}$ (hereafter named $Cdk8^{Camk2a}$), $Ankrd11^{Camk2a/Camk2a}$ (named hereafter $Ankrd11^{Camk2a}$), $Atp6ap2^{Camk2a/y}$, $Il1rapl1^{-/y}$, $Prps1^{Camk2a/y}$, $Ptchd1^{-/y}$, $Arx^{Dup24/y}$, and $Ascc3^{Camk2a/Camk2a}$ (hereafter named $Ascc3^{Camk2a}$). These eight mutant lines showed a substantial increase in locomotor activity and stereotypic behaviour in different situations including actimetric cages (increased number of beam-breaks), the open field (higher distance travelled over the 30 min test) (Figure 2), the Y-maze, and social tests (increased number of visits) [85,86]. They also showed other behavioural alterations. For example, all $Atp6ap2^{Camk2a/y}$ [85], $Il1rapl1^{-/y}$ and $Ptchd1^{-/y}$ [86] mutants had altered contextual and cued fear conditioning, displaying reduced percentage of freezing both during the context and the cued testing sessions (Figure 2). $Ankrd11^{Camk2a}$ also had decreased contextual fear conditioning. In addition, $Il1rapl1^{-/y}$ mice had altered spatial learning in the water maze with reduced number of platform crosses, while $Ptchd1^{-/y}$ had decreased working memory both in the Y-maze and the object recognition tasks [86] (Figure 2). They also showed altered motor abilities, evidenced by decreased muscle strength in $Ptchd1^{-/y}$ and $Cdk8^{Camk2a}$ mutants (Figure 2) and decreased startle response in the $Atp6ap2^{Camk2a/y}$ mice [85].

#### 3.1.2. Hypoactivity Group

Mutant lines constituting this group ($Ehmt1^{+/-}$, $Ehmt1^{+/-}/Ehmt2^{+/-}$, $Mbd5^{+/-}$, $Cdkl5^{-/y}$, $Mecp2^{-/y}$) showed decreased locomotor activity in the actimetric cages, in the social test and in the Y-maze evidenced by reduced number of beam breaks and reduced number of entries/visits (Figure 3). $Ehmt1^{+/-}$, $Ehmt1^{+/-}/Ehmt2^{+/-}$ and $Cdkl5^{-/y}$ mutants were also less active than their matched wildtypes in a novel environment in the open field, showing lower distance travelled than their corresponding wildtypes (Figure 3).

This group of hypoactive mutants also had other behavioural alterations. $Mbd5^{+/-}$ had decreased contextual and cued fear conditioning with decreased freezing performance, improved sociability exploring more the congener than an object, but had altered social memory displaying no preference of novel congener, and decreased startle response (Figure 4). On the other hand, $Ehmt1^{+/-}$, $Ehmt1^{+/-}/Ehmt2^{+/-}$ had altered recognition memory with recognition index around the chance level, altered social memory (for $Ehmt1^{+/-}$) and increased startle response (Figure 4). $Cdkl5^{-/y}$ displayed decreased prepulse inhibition (PPI) and increased thermal pain threshold (Figure 4), while $Mecp2^{-/y}$ mutants had decreased startle reactivity and PPI, showed substantial tremors (100% of accuracy), and had a decreased thermal pain threshold. Finally, all these hypoactive lines, except $Mecp2^{-/y}$, which showed the opposite phenotype, displayed a trend of increased anxiety with either decreased exploration of the centre of the open field during the first 5 min and decreased object exploration ($Ehmt1^{+/-}$, $Ehmt1^{+/-}/Ehmt2^{+/-}$) or increased latencies to exit the start arm in the Y-maze ($Mbd5^{+/-}$, $Cdkl5^{-/y}$) (Figure 4). $Mecp2^{-/y}$ mutants instead showed decreased marble burying, increased activity in the open field during the first 5 min, and increased open arm exploration in the elevated plus maze, reflected by increased head dips, tendency to increased percentage of time and decreased entry latency in the open arms.

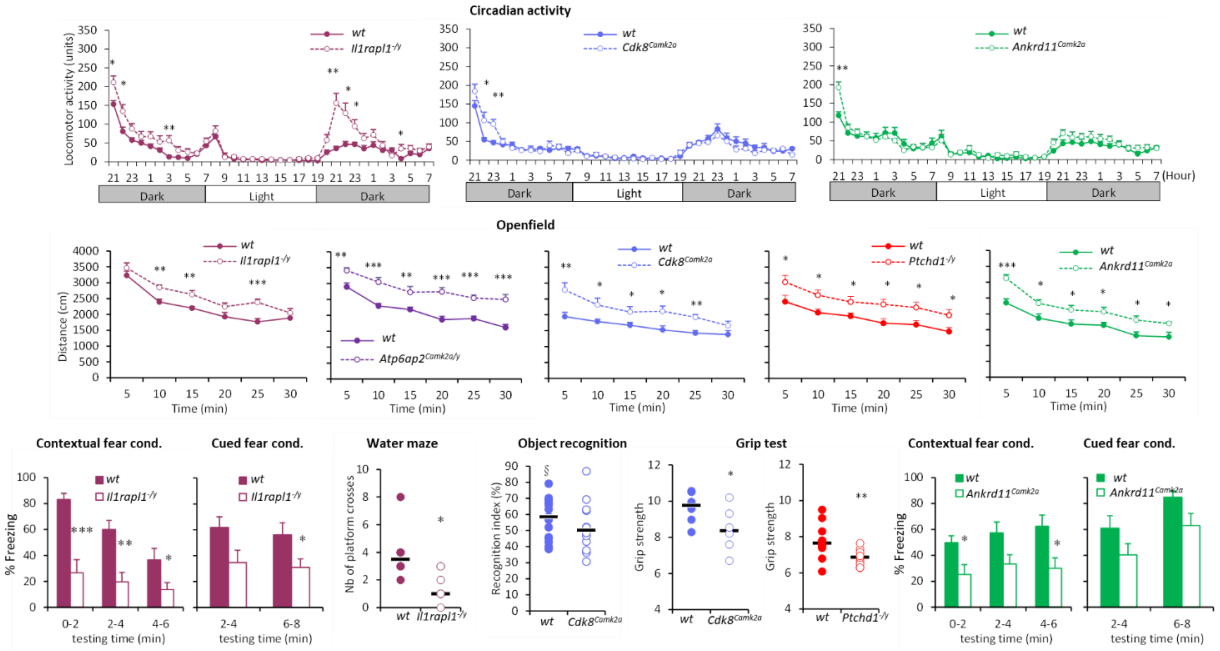


**Figure 2.** Selected behavioural alterations in the hyperactivity group. *Cdk8*$^{Camk2a}$, *Ankrd11*$^{Camk2a}$, *Atp6ap2*$^{Camk2a/y}$, *Ilrapl1*$^{-/y}$ and *Ptchd1*$^{-/y}$ [86] showed increased activity in the circadian activity and open field tests reflected by a higher number of beam breaks and distance travelled compared to wild-types. Data are expressed as the mean ±SEM of front and back successive beam breaks (circadian activity) and distance (open field) across time, and analysed using repeated measures ANOVA, followed by *t*-tests for each time point. *Cdk8*$^{Camk2a}$, *Ankrd11*$^{Camk2a}$, and *Ilrapl1*$^{-/y}$ showed altered learning performance in the water maze (decreased number of platform crosses for *Ilrapl1*$^{-/y}$), fear conditioning (decreased percentage of freezing for *Ankrd11*$^{Camk2a}$ and *Ilrapl1*$^{-/y}$) or object recognition (*Cdk8*$^{Camk2a}$), or motor deficits in the grip test (*Cdk8*$^{Camk2a}$ and *Ptchd1*$^{-/y}$). Data are expressed as mean ± SEM% freezing (fear conditioning), or scattergrams with the median for number of platform crosses (water maze), recognition index (object recognition), or muscle strength (grip test), and analysed using either repeated measures ANOVA followed by *t*-tests, or Student *t*-tests for single time points. * $p < 0.05$, ** $p < 0.01$, *** $p < 0.001$ vs. WT; § $p < 0.05$ vs. the chance level (only WT displayed good performance while mutants performed at the hazard level).

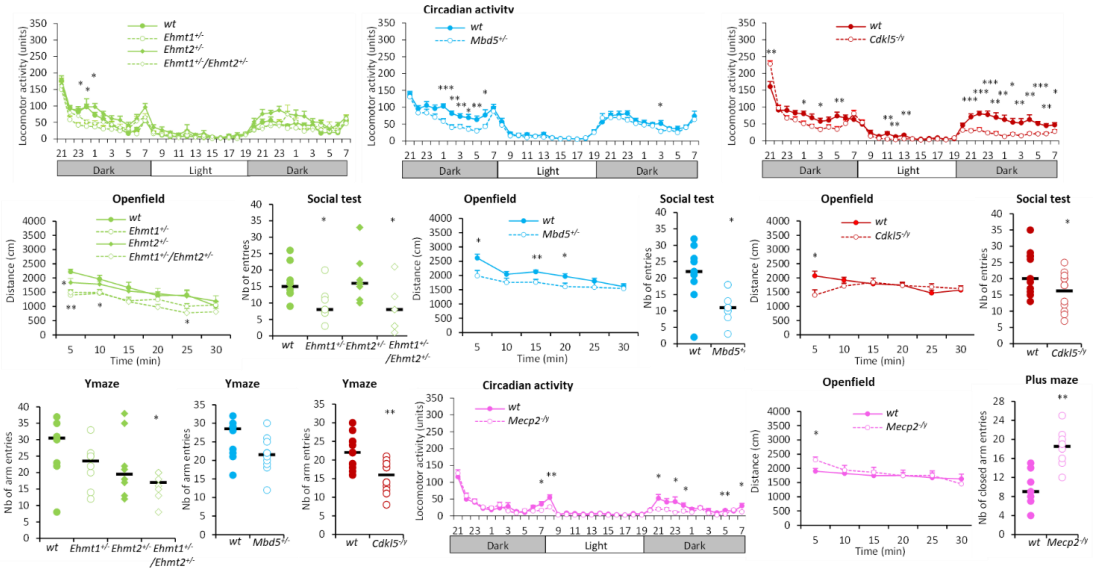


**Figure 3.** Hypoactivity group. *Ehmt1*$^{+/-}$, *Ehmt1*$^{+/-}$/*Ehmt2*$^{+/-}$, *Mbd5*$^{+/-}$ and *Cdkl5*$^{-/y}$ showed decreased activity in the circadian activity, in the open field, in social recognition and in the Y-maze

tests, reflected by lower number of beam breaks, reduced distance, and lower number of visits or arm entries, respectively, as compared to wild-type counterparts. *Mecp2*$^{-/y}$ showed decreased locomotion in circadian activity and increased closed arm entries in the elevated plus maze. Data are expressed as the mean ± SEM of front and back beam breaks (circadian activity) distance (open field) across time, or as scattergrams with the median for the number of entries (social, Y-maze, plus maze tests) and analysed using repeated measures ANOVA, followed by a *t*-test for each time point. * $p < 0.05$, ** $p < 0.01$, *** $p < 0.001$ vs. WT.

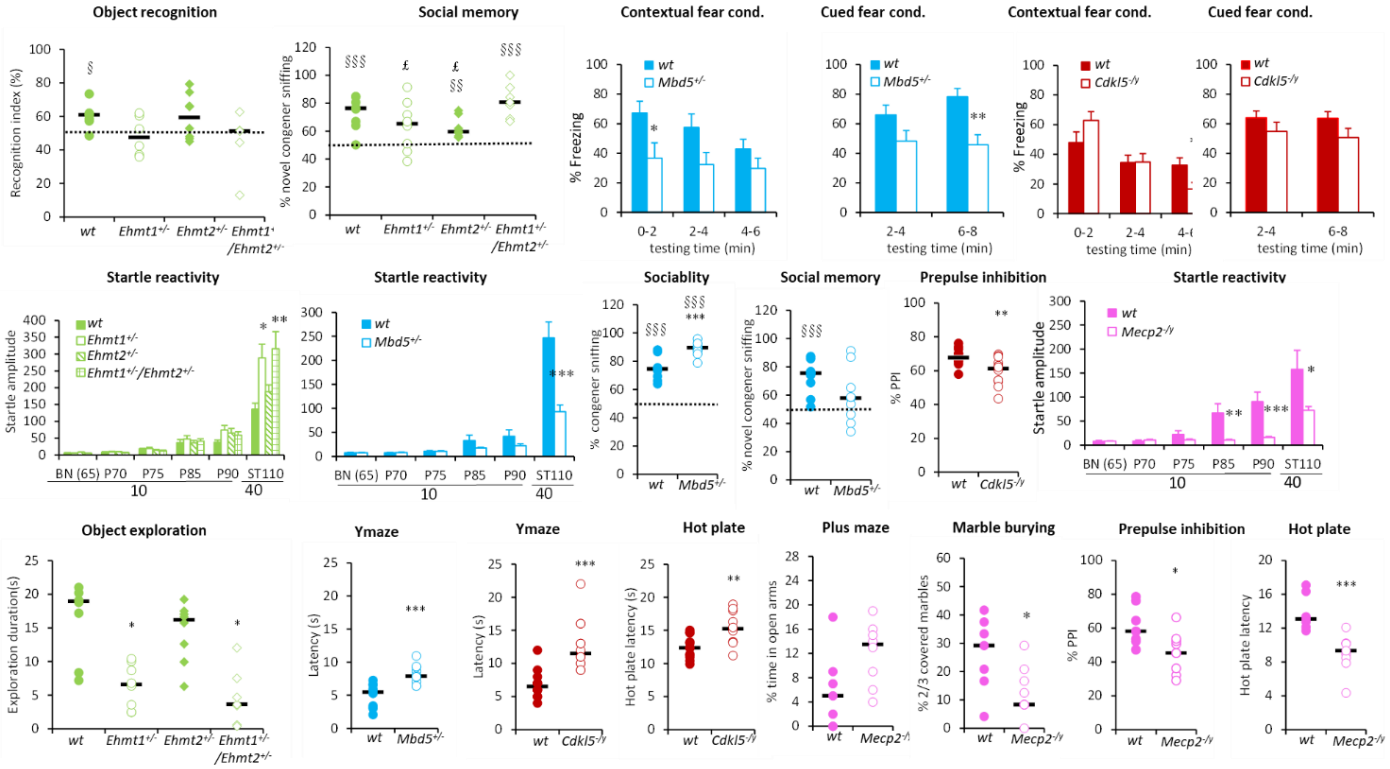


**Figure 4.** Selected behavioural alterations in the hypoactivity group. *Ehmt1*$^{+/-}$, *Ehmt1*$^{+/-}$/*Ehmt2*$^{+/-}$, *Mbd5*$^{+/-}$ showed altered memory performance in the fear conditioning (decreased % of freezing), object recognition (recognition index) or social tests (% novel congener sniffing). *Mbd5*$^{+/-}$ and *Mecp2*$^{-/y}$ had decreased startle while *Ehmt1*$^{+/-}$, *Ehmt1*$^{+/-}$/*Ehmt2*$^{+/-}$ had improved startle. *Ehmt1*$^{+/-}$, *Ehmt1*$^{+/-}$/*Ehmt2*$^{+/-}$, *Mbd5*$^{+/-}$ and *Cdkl5*$^{-/y}$ showed increased anxiety in the open field (decreased object exploration) or in the Y-maze (increased latency). Mecp2 mutants show decreased anxiety in marble burying (decreased number of marbles covered) and in the plus maze (increased %time in the open arms) and decreased pain threshold. Data are mean ± SEM (fear conditioning, startle reactivity) or scattergrams with the median (object recognition, social test, Y-maze, marble burying, hot plate). Data are analysed using either repeated measures ANOVA followed by *t*-tests or Student's *t*-test for single time points. * $p < 0.05$, ** $p < 0.01$, *** $p < 0.001$ vs. WT; § $p < 0.05$, §§ $p < 0.01$, §§§ $p < 0.001$ vs. the chance level; £ vs. *Ehmt1*$^{+/-}$/*Ehmt2*$^{+/-}$.

### 3.1.3. No Activity Phenotype Group

Finally, a group of mutant lines including *Nr1i3*$^{-/-}$, *Dyrk1a*$^{Camk2a}$, *Dyrk1a*$^{Dlx5,6/+}$, *Stard8*$^{-/y}$, *Wdr62*$^{-/-}$, *Kif5c*$^{+/-}$, *miR137*$^{+/-}$, and *Ehmt2*$^{+/-}$ did not show any strong pattern of modified activity and displayed only a limited number of behavioural changes.

## *3.2. PCA and Cluster Analysis*

Based on association studies, additional statistical analysis was performed on the 21 mutant lines whose genes are closely associated with ID (six genes were excluded). A graphical representation of phenotype scores was done using a heatmap combined with a

dendrogram showing the arrangement of mutant line clusters produced by hierarchical clustering (Figure 5 and Supplementary Materials). Correlated variables were grouped together on a circle of correlations. The smaller an individual coordinate on an axis, the smaller its contribution to the component. The three first components explained 70.27% of the variance (Figure 5A).

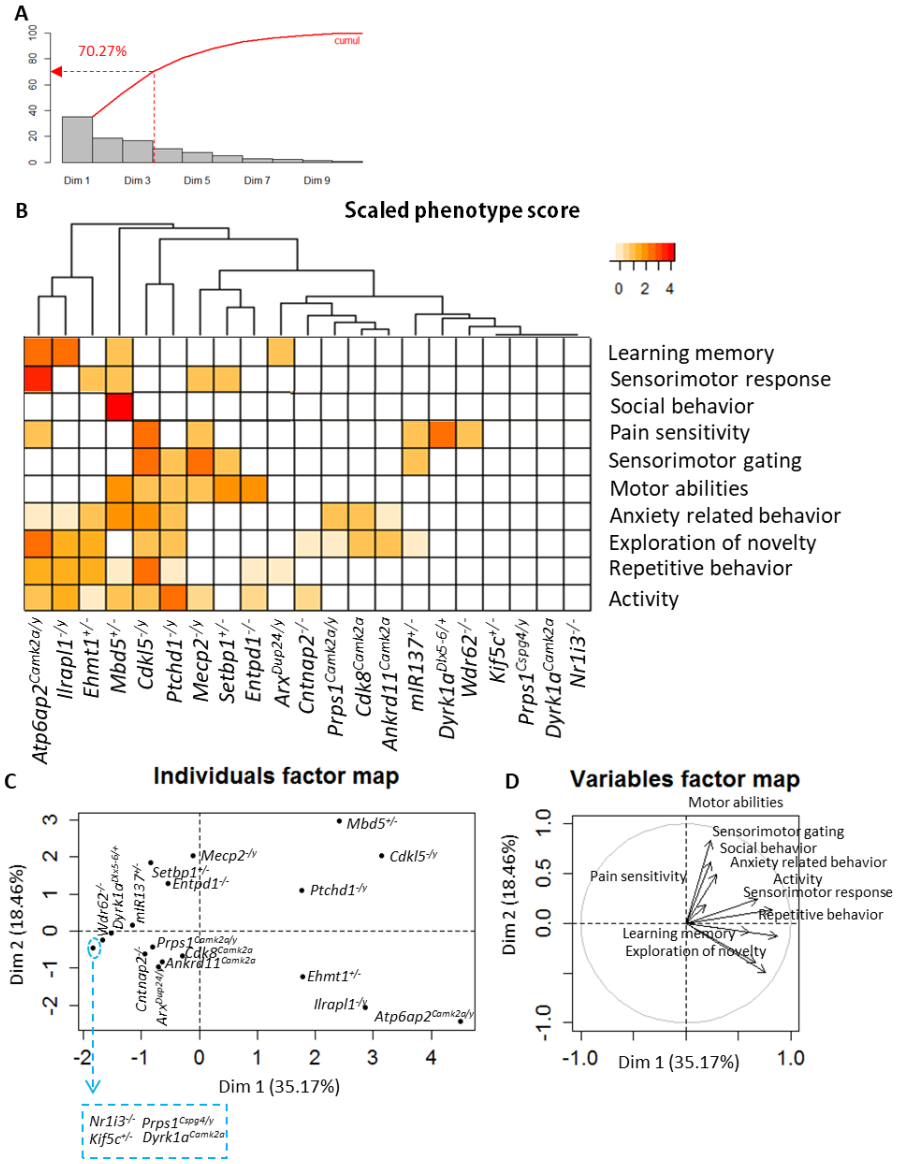


**Figure 5.** (**A**) PCA—Percentage of explained variance in principal component analysis for each component and cumulated percentage of explained variance. (**B**) Heatmap of scaled phenotype scores data. Row dendrograms show the distance between mutant lines and arrangement produced by hierarchical clustering. Colours indicate the phenotype score level. The darker the orange, the more phenotype parameters the biological function has. (**C**) PCA—Individuals factor map shows in axes 1 and 2 similarity of components between mutant lines. Note: 4 mutant lines listed in the blue square have the same coordinates. (**D**) PCA—Variables factor maps or correlations circle shows in axes 1 and 2 links between biological functions and the axes.

The first observation of Figure 5B shows a group of mutant lines, including *Atp6ap2*$^{Camk2a/y}$, *Il1rapl1*$^{-/y}$, *Ehmt1*$^{+/-}$, *Mbd5*$^{+/-}$, *Cdkl5*$^{-/y}$, and *Ptchd1*$^{-/y}$, with a high number of functional alterations. The second cluster includes gene mutations with a moderate number of altered functions, and includes *Mecp2*$^{-/y}$, *Setbp1*$^{+/-}$, *Entpd1*$^{-/-}$, *miR137*$^{+/-}$, *Dyrk1a*$^{Dlx5-6/+}$,

*Wdr62*$^{-/-}$, *Prps1*$^{Camk2a/y}$, *Cdk8*$^{Camk2a}$, *Ankrd11*$^{Camk2a}$, *Arx*$^{Dup24/y}$, and *Cntnap2*$^{-/-}$. The last group of mutants displayed a few changes or no phenotype. PCA was performed to visualise potential links between biological functions and mutant line similarities (Figure 5C,D and Supplementary Materials). On the one hand, a group of lines including *Cdkl5*$^{-/y}$, *Il1rapl1*$^{-/y}$, *Ptchd1*$^{-/y}$, *Atp6ap2*$^{Camk2a/y}$, *Mbd5*$^{+/-}$, and *Ehmt1*$^{+/-}$ displayed alterations mainly in activity, repetitive behaviour, novelty exploration and anxiety (Axis 1). On the other hand, mutant lines including *Cdk8*$^{Camk2a}$, *Mecp2*$^{-/y}$ and *Setbp1*$^{+/-}$ showed deficits in motor abilities and pain sensitivity, while *Atp6ap2*$^{Camk2a/y}$ and *Ilrapl1*$^{-/y}$ showed learning and memory deficits.

## 4. Discussion

In the present study, we generated 50 mutant lines for 45 genes clinically or potentially relevant for further understanding ID in humans. About 66% of the mutant lines generated were homozygous/hemizygous lethal, providing evidence that these genes are essential for normal development and survival. Embryonic phenotyping of homozygous/hemizygous/heterozygous lethal lines revealed several abnormalities, including pronounced craniofacial and skeletal defects, severe ganglia hypoplasia, and abnormal nervous or sensory system development in line with congenital malformations observed in the corresponding human syndromes. For example, we found that *Setbp1*$^{-/-}$ mutants displayed palatal and vertebral skeletal defects, reduced DRG and abnormal nasopharyngeal opening, reproducing some aspects of the SETBP1 Disorders (also known as Mental Retardation, Autosomal Dominant 29), characterized by ID and distinctive facial features [61,87]. We also found in adult *Setbp1*$^{+/-}$ mice several behavioural alterations including muscle weakness and altered PPI reminiscent of symptoms observed in patients with a similar mutation type [88]. This model is of interest for better understanding the physiopathology of this new syndrome. Our results from *Med25*$^{-/-}$ embryos revealed several abnormalities including exencephaly, anophthalmia or cyclopia and telencephalon hypoplasia, in line with those observed in humans with *MED25* mutations such as Basel-Vanagaite-Smirin-Yosef syndrome characterized by severely delayed psychomotor development resulting in ID, as well as variable eye, brain, cardiac, and palatal abnormalities [47]. Our results obtained for *Tubb3*$^{M388V/+}$ embryos are in line with those previously reported for the *Tubb3*$^{R262C/R262C}$ mouse model and with a spectrum of abnormalities including hypoplasia of oculomotor nerves and dysgenesis of the corpus callosum and anterior commissure observed in human syndromes with TUBB3 mutations [66,67,89], supporting the role of TUBB3 in axonal guidance and maintenance.

Large scale standardized behavioural phenotyping of 27 mutant lines carrying mutations in genes involved in ID in humans revealed unique gene/phenotype behavioural profiles based on activity patterns. Interestingly, genes mutated in the hypoactive group are altered either in Kleefstra syndrome (*Ehmt1, Mbd5, Nr1i3*) or Rett syndrome (*Mecp2*) or CDKL5 Deficiency Disorder, CDD (*Cdkl5)*. Kleefstra syndrome is characterized by ID, childhood hypotonia, severe expressive speech delay and a distinctive facial appearance with a spectrum of additional clinical features including autistic-like behavioural problems and cardiac defects [25,26,50,90]. Autosomal Dominant Mental Retardation 1/2q23.1 deletion syndrome, caused by pathogenic *MBD5* variants, shares several phenotypic traits with Kleefstra syndrome [36,37]. Similarly, patients with a pathogenic variant in *CDKL5* (CDKL5 Deficiency Disorder, CDD) or *MECP2* (Rett syndrome) present with overlapping clinical features.

We report here that *Ehmt1*$^{+/-}$, *Ehmt1*$^{+/-}$/*Ehmt2*$^{+/-}$ and *Mbd5*$^{+/-}$ mice show hypoactivity and learning and memory deficits in several situations, extending previously reported data in *Ehmt1*$^{+/-}$ mice [72,91], and recapitulating several cognitive, autistic and hypoactivity features observed in Kleefstra syndrome and 2q23.1 deletion patients, supporting the use of *Ehmt1*$^{+/-}$ and *Mbd5*$^{+/-}$ as good mammalian models for Kleefstra and Autosomal Dominant Mental Retardation 1/2q23.1 deletion syndromes.

We found only limited and weak behavioural changes in *Ehmt2*$^{+/-}$ and *Nr1i3*$^{-/-}$ mutants. *EHMT2* and its paralog *EHMT1* encodes a histone methyltransferase and act together in protein complexes responsible for deposition of mono- and di-methylated forms of Histone 3 Lysine 9 (H3K9me/me2). These methylation marks are associated with gene silencing in euchromatin [92]. Since LoF variants in *EHMT1* give rise to Kleefstra syndrome, it is tempting to speculate that *EHMT2* is a candidate for syndromic ID as well. However, our data from *Ehmt1*$^{+/-}$, *Ehm2*$^{+/-}$ and *Ehmt1*$^{+/-}$/*Ehmt2*$^{+/-}$ mutants show that the main phenotypic traits are linked to the *Ehmt1*$^{+/-}$ mutation, in line with a previous study where we showed that unlike *Ehmt1*$^{+/-}$, *Ehmt2*$^{+/-}$ did not present the marked increase of H3K9me2/3 [76] reduces the strength of the hypothesis linking *EHMT2* with Kleefstra spectrum disorders and is potentially associated ID. Indeed, several *EHMT2* LoF alleles have been reported without convincing evidence for involvement in human genetic disorders. For *NRI3*, a single de novo missense mutation (c.740T>C [p.Phe247Ser]) was identified in a patient with core symptoms of Kleefstra syndrome [50]. In our study, *Nr1i3*$^{-/-}$ mice displayed only a slight decrease in contextual fear conditioning. In line with behavioural data, the assessment of hippocampal neuronal morphology in *Nr1i3*$^{-/-}$ mice did not reveal any gross abnormality concerning neurite length, branching or excitatory synapse density (not shown). Elsewhere, the quantification of ectopic wing vein formation in Drosophila [50] revealed that the EHMT overexpression phenotype was almost completely rescued by heterozygous LoF mutations in *EcR/Nr1i3*, and overexpression of *EcR/Nr1i3* enhanced EHMT-induced ectopic vein formation, providing strong evidence of a synergistic relationship between EHMT and EcR/NR1I3, and that *NR1I3* per se has reduced incidence. Combined, the results could suggest that in the patient affected, the (c.740T>C [p.Phe247Ser]) single amino acid substitution is not a loss of function mutation and has a different effect on the protein. Additionally, the patient carried a de novo *MTMR9* missense variant (c.310T>G [p.(Ser104Ala)]; NM_015458.3) of uncertain significance [50].

Several mutant lines showed a characteristic hyperactivity phenotype. *Il1rapl1*$^{-/y}$, *Ptchd1*$^{-/y}$, and *Arx*$^{Dup24/y}$ mice displayed substantial hyperactivity and stereotypic behaviour, and either increased exploration or reduced anxiety. These mutant lines also had altered learning and memory abilities. In humans, *IL1RAPL1* and *PTCHD1* mutations are found in X-linked ID or X-linked autism spectrum disorders [32,58,59]. Among behavioural features of these syndromes, hyperactivity, stereotypies, and altered learning abilities are commonly present. Interestingly, motor problems including psychomotor delay and hypotonia present in patients with *PTCHD1* or *ARX* mutations were also found in our mutants, which displayed either decreased muscle strength (*Ptchd1*$^{-/y}$) or altered grasping and reaching, reflecting fine-tuned motor abilities (*Arx*$^{Dup24/y}$) [9,10,93]. In human syndromes, mutations are hemizygous substitutions or deletions (*IL1RAPL1*), hemizygous deletion or insertion (*PTCHD1*), or hemizygous c.428_451dup24 duplication (ARX). Our mutant lines reproduced some of these mutation types.

Mutations in *ANKRD11*, *ATP6AP2* and *PRPS1* have also been associated with several neurodevelopmental disorders with ID in humans [7,11,94,95]. *ATP6AP2* mutations are found in X-linked ID with Parkinsonism and spasticity, and *PRPS1* mutations in Arts syndrome, X-linked recessive Charcot-Marie-Tooth disease 5 and X-linked non-syndromic hearing loss [11,55–57,95–98]. Mutations are either hemizygous splice site mutations that leads to a LoF (*ATP6AP2*), or substitutions leading mainly to GoF, but also to LoF (*PRPS1*), causing different behavioural symptoms including hyperactivity, stereotypies and altered cognitive abilities. On the other hand, heterozygous deletions or splice site mutations in the *ANKRD11* gene have been found in patients with KBG syndrome, characterized by macrodontia, distinctive craniofacial and skeletal anomalies, short stature, and neurological problems including ID [7,94]. Hyperactivity, anxiety, and hearing loss have also been described [99]. In the present study, we generated *Atp6ap2*$^{-/y}$, *Prps1*$^{-/y}$ and *Ankrd11*$^{-/-}$ mutant lines and found them embryonic lethal. We then generated and characterized the neuronal specific lines *Ankrd11*$^{Camk2a}$, *Atp6ap2*$^{Camk2a/y}$, and *Prps1*$^{Camk2a/y}$. *Ankrd11*$^{Camk2a}$ and *Atp6ap2*$^{Camk2a/y}$ displayed substantial hyperactivity and stereotypic behaviour, in-

creased exploration and reduced anxiety, and altered learning and memory. Interestingly, *Atp6ap2*$^{Camk2a/y}$ also showed decreased startle response in line with motor problems including hypotonia found in patients. Our data reproduced some of the behavioural phenotypes observed in patients and support, at least in part, the specific effect of the deletion on excitatory neuronal cells. *Ankrd11*$^{+/-}$ mutants also showed hearing loss displaying increased ABR thresholds [100], in line with hearing problems reported in some KBG patients [99]. Among the hyperactive lines, *Prps1*$^{Camk2a/y}$ showed only subtle phenotypes displaying increased stereotypic behaviour and increased working memory. We assume that neuronal loss-of-function per se is unlikely to model syndrome-related behavioural traits. In line with this observation, we found that *Prps1*$^{Csp4/y}$ mice, a glial specific conditional KO, displayed increased stereotypic behaviour during the initial exploration in the actimetric cages, and decreased motor performance in the rotarod (Table S1).

In the present study we also analysed the effect of LoF variants in several candidate ID genes. One of these genes, *CDK8*, encodes an important regulator of the multi-subunit Mediator complex, involved in transcriptional processes. Mutations in other subunits of the Mediator complex were previously identified in syndromic and non-syndromic ID. *Cdk8*$^{-/-}$ mice are lethal; therefore, we generated and analysed *Cdk8*$^{Camk2a}$ mice. These mutants displayed hyperactivity in several situations, a trend to increased stereotypic behaviour, hypotonia reflected by decreased muscle strength, and altered recognition memory. While our studies were ongoing, various heterozygous *CDK8* missense mutations were reported to cause a syndromic developmental disorder characterized by hypotonia, ID, and behavioural abnormalities [13]. Affected individuals tended to have learning disability, autistic features and attention deficit-hyperactivity disorder (ADHD). In vitro functional studies showed that the mutations strongly attenuated CDK8 kinase activity, supporting a dominant-negative mechanism of pathogenesis for *CDK8* substitutions [13]. Interestingly, our data clearly recapitulate most behavioural alterations described in humans [13], and suggest that these alterations are neuronal specific.

*ASCC3* was identified as a candidate gene for autosomal recessive ID, with a potentially pathogenic missense variant (p.(S1564P)) identified in a single family [3]. In the present study, we show that *Ascc3*$^{-/-}$ mice are lethal, and *Ascc3*$^{Camk2a}$ mutants showed hyperactive behaviour and increased rearing in the actimetric cages, and reduced anxiety-related behaviour in the elevated plus maze. We suggest that neuronal homozygote deletion of *Ascc3* gene is not sufficient to induce profound behavioural alterations. The family affected by the *ASCC3* variant was also reported to have mild ID [3].

Across this study, applying an extensive behavioural pipeline allowed us to identify different classes of genes for which mutations caused several behavioural alterations. The heterogeneity of phenotypes and penetrance are reminiscent of the effects of mutations observed in human syndromes with ID. The class of genes with increased activity includes several *Camk2a*-conditional KO lines specific to excitatory neurons. It can be suggested that the hyperactive phenotype might be due, at least in part, to the *Camk2a* promoter driving Cre recombinase. Hyperactivity and stereotypies are almost common phenotypes in human syndromes with ID. In addition, our constitutive *Il1rapl1*$^{-/y}$ and *Ptchd1*$^{-/y}$, and *Arx*$^{Dup24/y}$ mice also showed substantial hyperactivity in different situations. Finally, behavioural phenotyping of the *Camk2a-Cre* reporter line did not show any obvious sign of hyperactivity or another relevant behavioural alteration (not shown). These arguments reduce the strength of the hypothesis that hyperactivity observed in the *Camk2a-mutant* lines is likely related to the *Camk2a* promoter driving Cre recombinase. Nevertheless, it is noteworthy that *Camk2-Cre* specific mutations for constitutively lethal lines are partially expressed (in the glutamatergic neurons). Additional data from mutants bred on other reporter lines would increase our knowledge about the effect of mutations described in this study depending on their expression in other cellular compartments. Conditional mutants with combined expression in different cell types might potentially display extensive or stronger phenotypic traits affecting more functions.

Our functional findings are based on a thorough behavioural exploration of gene mutations related to ID in mice, focussing on males. It should be emphasized that around 33% of genes involved in ID (and those generated here) are X-linked genes. That is the main reason why only males were characterized in this study, although this might also be considered a limitation. The extension of phenotyping to females might have increased the strength of our findings. In this regard, in the context of another worldwide effort designed to generate and characterize null mouse models for all the genes of the mouse genome, we also characterized mutant females with some of the genes from the present collection. For example, *Ptchd1*$^{-/-}$ females also displayed several behavioural abnormalities including hyperactivity and cognitive deficits, extending the data observed in *Ptchd1*$^{-/y}$ males [86].

## 5. Conclusions

The results of the present study allowed us to establish a broad gene-phenotype relationship map for a wide range of genes involved in several neurodevelopmental disorders with ID, or potentially involved in ID. Several of the mutant lines studied reproduced, as far as possible, the human mutation types, and displayed strong phenotypic similarities with patient features, constituting interesting genetic tools to better understand human syndromes with ID and making it possible to establish new potential therapeutic strategies.

**Supplementary Materials:** The following supporting information can be downloaded at: https://www.mdpi.com/article/10.3390/biomedicines10123148/s1. Figure S1: Mouse models generated and phenotyped in the Gencodys consortium; Figure S2: Cranial and cervical vertebra abnormalities of Setbp1$^{-/-}$ mice at E15.5 and E18.5; Figure S3: Cranial nerve and associated ganglia, as well as dorsal root ganglia abnormalities in Tubb3M388V/M388V mutant embryos; Figure S4: Severe craniofacial abnormalities in Med25$^{-/-}$ mutant embryos and fetuses; Table S1: Gene/phenotype heatmap drawn from main parameters of different tests from 27 characterized mutant lines; Table S2: Biological function categories and related parameters, established for PCA analysis and cluster representation; Table S3: The phenotype scores calculated for each mutant line and functional category to perform PCA analysis and cluster representation.

**Author Contributions:** H.v.B., J.C., P.B., F.L., V.M.K. and Y.H. selected the genes of interest. H.M. and Y.H. conceived the study and wrote the manuscript. M.-C.B. and G.P. designed the mouse lines. M.S. and T.S. produced phenotyping cohorts. H.M. and O.W. carried out further analysis of behavioural and embryo data, S.L. performed bioinformatic analysis. P.B., F.L., A.D. and V.M.K. contributed by reading the manuscript. H.v.B., J.C., P.B., FL., V.M.K. and Y.H. supervised the project, and secured the funding. All authors have read and agreed to the published version of the manuscript.

**Funding:** This work was supported by the European Union (FP7 Gencodys, grant 241995), the University of Strasbourg (Unistra), the National Centre for Scientific Research (CNRS), the French National Institute of Health and Medical Research (INSERM), French government funds through the "Agence Nationale de la Recherche" in the framework of the Investissements d'Avenir program by IdEx Unistra (ANR-10-IDEX-0002), a SFRI-STRAT'US project (ANR 20-SFRI-0012) and EUR IMCBio (ANR-17-EURE-0023) and INBS PHENOMIN (ANR-10-IDEX-0002-02). The funders had no role in study design, data collection and analysis, decision to publish, or preparation of the manuscript.

**Institutional Review Board Statement:** The procedures carried out in this project were performed in agreement with EC directive 2010/63/UE86/609/CEE, submitted to the French ethics committee 017 (Com'Eth) and received the accreditation under the number 2012-139.

**Data Availability Statement:** The data presented in this study are available upon request.

**Acknowledgments:** Behavioural phenotyping was performed by the Phenomin-ICS behavioural team staff, particularly Valérie Lalanne and Christophe Mittelhaeuser. We would like to thank Jean-Louis Mandel for our discussion during the program and for his comments on the manuscript, Laurent Vasseur for his contribution to the information database, Hugues Jacobs and Fabien Pertuy for the acquisition and 3D reconstruction of embryos, and the members of Phenomin-ICS animal facility for breeding, care, and genotyping of mice from the different cohorts.

**Conflicts of Interest:** The authors declare no conflict of interest.

## References


1. Ilyas, M.; Mir, A.; Efthymiou, S.; Houlden, H. The genetics of intellectual disability: Advancing technology and gene editing. *F1000Research* **2020**, *9*, 22. [CrossRef] [PubMed]
2. Kochinke, K.; Zweier, C.; Nijhof, B.; Fenckova, M.; Cizek, P.; Honti, F.; Keerthikumar, S.; Oortveld, M.A.; Kleefstra, T.; Kramer, J.M.; et al. Systematic Phenomics Analysis Deconvolutes Genes Mutated in Intellectual Disability into Biologically Coherent Modules. *Am. J. Hum. Genet.* **2016**, *98*, 149–164. [CrossRef]
3. Najmabadi, H.; Hu, H.; Garshasbi, M.; Zemojtel, T.; Abedini, S.S.; Chen, W.; Hosseini, M.; Behjati, F.; Haas, S.; Jamali, P.; et al. Deep sequencing reveals 50 novel genes for recessive cognitive disorders. *Nature* **2011**, *478*, 57–63. [CrossRef] [PubMed]
4. Twigg, S.R.; Matsumoto, K.; Kidd, A.M.; Goriely, A.; Taylor, I.B.; Fisher, R.B.; Hoogeboom, A.J.; Mathijssen, I.M.; Lourenco, M.T.; Morton, J.E.; et al. The origin of EFNB1 mutations in craniofrontonasal syndrome: Frequent somatic mosaicism and explanation of the paucity of carrier males. *Am. J. Hum. Genet.* **2006**, *78*, 999–1010. [CrossRef] [PubMed]
5. Wieland, I.; Weidner, C.; Ciccone, R.; Lapi, E.; McDonald-McGinn, D.; Kress, W.; Jakubiczka, S.; Collmann, H.; Zuffardi, O.; Zackai, E.; et al. Contiguous gene deletions involving EFNB1, OPHN1, PJA1 and EDA in patients with craniofrontonasal syndrome. *Clin. Genet.* **2007**, *72*, 506–516. [CrossRef]
6. Billuart, P.; Bienvenu, T.; Ronce, N.; des Portes, V.; Vinet, M.C.; Zemni, R.; Roest Crollius, H.; Carrie, A.; Fauchereau, F.; Cherry, M.; et al. Oligophrenin-1 encodes a rhoGAP protein involved in X-linked mental retardation. *Nature* **1998**, *392*, 923–926. [CrossRef] [PubMed]
7. Sirmaci, A.; Spiliopoulos, M.; Brancati, F.; Powell, E.; Duman, D.; Abrams, A.; Bademci, G.; Agolini, E.; Guo, S.; Konuk, B.; et al. Mutations in ANKRD11 cause KBG syndrome, characterized by intellectual disability, skeletal malformations, and macrodontia. *Am. J. Hum. Genet.* **2011**, *89*, 289–294. [CrossRef] [PubMed]
8. Stromme, P.; Mangelsdorf, M.E.; Shaw, M.A.; Lower, K.M.; Lewis, S.M.; Bruyere, H.; Lutcherath, V.; Gedeon, A.K.; Wallace, R.H.; Scheffer, I.E.; et al. Mutations in the human ortholog of Aristaless cause X-linked mental retardation and epilepsy. *Nat. Genet.* **2002**, *30*, 441–445. [CrossRef]
9. Curie, A.; Nazir, T.; Brun, A.; Paulignan, Y.; Reboul, A.; Delange, K.; Cheylus, A.; Bertrand, S.; Rochefort, F.; Bussy, G.; et al. The c.429_452 duplication of the ARX gene: A unique developmental-model of limb kinetic apraxia. *Orphanet J. Rare Dis.* **2014**, *9*, 25. [CrossRef]
10. Dubos, A.; Meziane, H.; Iacono, G.; Curie, A.; Riet, F.; Martin, C.; Loaec, N.; Birling, M.C.; Selloum, M.; Normand, E.; et al. A new mouse model of ARX dup24 recapitulates the patients' behavioral and fine motor alterations. *Hum. Mol. Genet.* **2018**, *27*, 2138–2153. [CrossRef]
11. Ramser, J.; Abidi, F.E.; Burckle, C.A.; Lenski, C.; Toriello, H.; Wen, G.; Lubs, H.A.; Engert, S.; Stevenson, R.E.; Meindl, A.; et al. A unique exonic splice enhancer mutation in a family with X-linked mental retardation and epilepsy points to a novel role of the renin receptor. *Hum. Mol. Genet.* **2005**, *14*, 1019–1027. [CrossRef] [PubMed]
12. Korvatska, O.; Strand, N.S.; Berndt, J.D.; Strovas, T.; Chen, D.H.; Leverenz, J.B.; Kiianitsa, K.; Mata, I.F.; Karakoc, E.; Greenup, J.L.; et al. Altered splicing of ATP6AP2 causes X-linked parkinsonism with spasticity (XPDS). *Hum. Mol. Genet.* **2013**, *22*, 3259–3268. [CrossRef]
13. Calpena, E.; Hervieu, A.; Kaserer, T.; Swagemakers, S.M.A.; Goos, J.A.C.; Popoola, O.; Ortiz-Ruiz, M.J.; Barbaro-Dieber, T.; Bownass, L.; Brilstra, E.H.; et al. De Novo Missense Substitutions in the Gene Encoding CDK8, a Regulator of the Mediator Complex, Cause a Syndromic Developmental Disorder. *Am. J. Hum. Genet.* **2019**, *104*, 709–720. [CrossRef] [PubMed]
14. Kalscheuer, V.M.; Tao, J.; Donnelly, A.; Hollway, G.; Schwinger, E.; Kubart, S.; Menzel, C.; Hoeltzenbein, M.; Tommerup, N.; Eyre, H.; et al. Disruption of the serine/threonine kinase 9 gene causes severe X-linked infantile spasms and mental retardation. *Am. J. Hum. Genet.* **2003**, *72*, 1401–1411. [CrossRef]
15. Weaving, L.S.; Christodoulou, J.; Williamson, S.L.; Friend, K.L.; McKenzie, O.L.; Archer, H.; Evans, J.; Clarke, A.; Pelka, G.J.; Tam, P.P.; et al. Mutations of CDKL5 cause a severe neurodevelopmental disorder with infantile spasms and mental retardation. *Am. J. Hum. Genet.* **2004**, *75*, 1079–1093. [CrossRef] [PubMed]
16. Strauss, K.A.; Puffenberger, E.G.; Huentelman, M.J.; Gottlieb, S.; Dobrin, S.E.; Parod, J.M.; Stephan, D.A.; Morton, D.H. Recessive symptomatic focal epilepsy and mutant contactin-associated protein-like 2. *N. Engl. J. Med.* **2006**, *354*, 1370–1377. [CrossRef]
17. Zweier, C.; de Jong, E.K.; Zweier, M.; Orrico, A.; Ousager, L.B.; Collins, A.L.; Bijlsma, E.K.; Oortveld, M.A.; Ekici, A.B.; Reis, A.; et al. CNTNAP2 and NRXN1 are mutated in autosomal-recessive Pitt-Hopkins-like mental retardation and determine the level of a common synaptic protein in Drosophila. *Am. J. Hum. Genet.* **2009**, *85*, 655–666. [CrossRef] [PubMed]
18. Vernes, S.C.; Newbury, D.F.; Abrahams, B.S.; Winchester, L.; Nicod, J.; Groszer, M.; Alarcon, M.; Oliver, P.L.; Davies, K.E.; Geschwind, D.H.; et al. A functional genetic link between distinct developmental language disorders. *N. Engl. J. Med.* **2008**, *359*, 2337–2345. [CrossRef]
19. Xu, G.L.; Bestor, T.H.; Bourc'his, D.; Hsieh, C.L.; Tommerup, N.; Bugge, M.; Hulten, M.; Qu, X.; Russo, J.J.; Viegas-Pequignot, E. Chromosome instability and immunodeficiency syndrome caused by mutations in a DNA methyltransferase gene. *Nature* **1999**, *402*, 187–191. [CrossRef] [PubMed]
20. Hansen, R.S.; Wijmenga, C.; Luo, P.; Stanek, A.M.; Canfield, T.K.; Weemaes, C.M.; Gartler, S.M. The DNMT3B DNA methyltransferase gene is mutated in the ICF immunodeficiency syndrome. *Proc. Natl. Acad. Sci. USA* **1999**, *96*, 14412–14417. [CrossRef]

21. Weedon, M.N.; Hastings, R.; Caswell, R.; Xie, W.; Paszkiewicz, K.; Antoniadi, T.; Williams, M.; King, C.; Greenhalgh, L.; Newbury-Ecob, R.; et al. Exome sequencing identifies a DYNC1H1 mutation in a large pedigree with dominant axonal Charcot-Marie-Tooth disease. *Am. J. Hum. Genet.* **2011**, *89*, 308–312. [CrossRef] [PubMed]
22. Poirier, K.; Lebrun, N.; Broix, L.; Tian, G.; Saillour, Y.; Boscheron, C.; Parrini, E.; Valence, S.; Pierre, B.S.; Oger, M.; et al. Mutations in TUBG1, DYNC1H1, KIF5C and KIF2A cause malformations of cortical development and microcephaly. *Nat. Genet.* **2013**, *45*, 639–647. [CrossRef]
23. Harms, M.B.; Ori-McKenney, K.M.; Scoto, M.; Tuck, E.P.; Bell, S.; Ma, D.; Masi, S.; Allred, P.; Al-Lozi, M.; Reilly, M.M.; et al. Mutations in the tail domain of DYNC1H1 cause dominant spinal muscular atrophy. *Neurology* **2012**, *78*, 1714–1720. [CrossRef] [PubMed]
24. Moller, R.S.; Kubart, S.; Hoeltzenbein, M.; Heye, B.; Vogel, I.; Hansen, C.P.; Menzel, C.; Ullmann, R.; Tommerup, N.; Ropers, H.H.; et al. Truncation of the Down syndrome candidate gene DYRK1A in two unrelated patients with microcephaly. *Am. J. Hum. Genet.* **2008**, *82*, 1165–1170. [CrossRef] [PubMed]
25. Kleefstra, T.; Smidt, M.; Banning, M.J.; Oudakker, A.R.; Van Esch, H.; de Brouwer, A.P.; Nillesen, W.; Sistermans, E.A.; Hamel, B.C.; de Bruijn, D.; et al. Disruption of the gene Euchromatin Histone Methyl Transferase1 (Eu-HMTase1) is associated with the 9q34 subtelomeric deletion syndrome. *J. Med. Genet.* **2005**, *42*, 299–306. [CrossRef] [PubMed]
26. Kleefstra, T.; Brunner, H.G.; Amiel, J.; Oudakker, A.R.; Nillesen, W.M.; Magee, A.; Genevieve, D.; Cormier-Daire, V.; van Esch, H.; Fryns, J.P.; et al. Loss-of-function mutations in euchromatin histone methyl transferase 1 (EHMT1) cause the 9q34 subtelomeric deletion syndrome. *Am. J. Hum. Genet.* **2006**, *79*, 370–377. [CrossRef] [PubMed]
27. Novarino, G.; Fenstermaker, A.G.; Zaki, M.S.; Hofree, M.; Silhavy, J.L.; Heiberg, A.D.; Abdellateef, M.; Rosti, B.; Scott, E.; Mansour, L.; et al. Exome sequencing links corticospinal motor neuron disease to common neurodegenerative disorders. *Science* **2014**, *343*, 506–511. [CrossRef] [PubMed]
28. Hu, H.; Haas, S.A.; Chelly, J.; Van Esch, H.; Raynaud, M.; de Brouwer, A.P.; Weinert, S.; Froyen, G.; Frints, S.G.; Laumonnier, F.; et al. X-exome sequencing of 405 unresolved families identifies seven novel intellectual disability genes. *Mol. Psychiatry* **2016**, *21*, 133–148. [CrossRef] [PubMed]
29. Matosin, N.; Green, M.J.; Andrews, J.L.; Newell, K.A.; Fernandez-Enright, F. Possibility of a sex-specific role for a genetic variant in FRMPD4 in schizophrenia, but not cognitive function. *Neuroreport* **2016**, *27*, 33–38. [CrossRef]
30. de Ligt, J.; Willemsen, M.H.; van Bon, B.W.; Kleefstra, T.; Yntema, H.G.; Kroes, T.; Vulto-van Silfhout, A.T.; Koolen, D.A.; de Vries, P.; Gilissen, C.; et al. Diagnostic exome sequencing in persons with severe intellectual disability. *N. Engl. J. Med.* **2012**, *367*, 1921–1929. [CrossRef]
31. Carrie, A.; Jun, L.; Bienvenu, T.; Vinet, M.C.; McDonell, N.; Couvert, P.; Zemni, R.; Cardona, A.; Van Buggenhout, G.; Frints, S.; et al. A new member of the IL-1 receptor family highly expressed in hippocampus and involved in X-linked mental retardation. *Nat. Genet.* **1999**, *23*, 25–31. [CrossRef] [PubMed]
32. Piton, A.; Michaud, J.L.; Peng, H.; Aradhya, S.; Gauthier, J.; Mottron, L.; Champagne, N.; Lafreniere, R.G.; Hamdan, F.F.; S2D team; et al. Mutations in the calcium-related gene IL1RAPL1 are associated with autism. *Hum. Mol. Genet.* **2008**, *17*, 3965–3974. [CrossRef] [PubMed]
33. Koolen, D.A.; Kramer, J.M.; Neveling, K.; Nillesen, W.M.; Moore-Barton, H.L.; Elmslie, F.V.; Toutain, A.; Amiel, J.; Malan, V.; Tsai, A.C.; et al. Mutations in the chromatin modifier gene KANSL1 cause the 17q21.31 microdeletion syndrome. *Nat. Genet.* **2012**, *44*, 639–641. [CrossRef] [PubMed]
34. Jensen, L.R.; Amende, M.; Gurok, U.; Moser, B.; Gimmel, V.; Tzschach, A.; Janecke, A.R.; Tariverdian, G.; Chelly, J.; Fryns, J.P.; et al. Mutations in the JARID1C gene, which is involved in transcriptional regulation and chromatin remodeling, cause X-linked mental retardation. *Am. J. Hum. Genet.* **2005**, *76*, 227–236. [CrossRef] [PubMed]
35. Alazami, A.M.; Al-Owain, M.; Alzahrani, F.; Shuaib, T.; Al-Shamrani, H.; Al-Falki, Y.H.; Al-Qahtani, S.M.; Alsheddi, T.; Colak, D.; Alkuraya, F.S. Loss of function mutation in LARP7, chaperone of 7SK ncRNA, causes a syndrome of facial dysmorphism, intellectual disability, and primordial dwarfism. *Hum. Mutat.* **2012**, *33*, 1429–1434. [CrossRef] [PubMed]
36. Wagenstaller, J.; Spranger, S.; Lorenz-Depiereux, B.; Kazmierczak, B.; Nathrath, M.; Wahl, D.; Heye, B.; Glaser, D.; Liebscher, V.; Meitinger, T.; et al. Copy-number variations measured by single-nucleotide-polymorphism oligonucleotide arrays in patients with mental retardation. *Am. J. Hum. Genet.* **2007**, *81*, 768–779. [CrossRef] [PubMed]
37. Williams, S.R.; Mullegama, S.V.; Rosenfeld, J.A.; Dagli, A.I.; Hatchwell, E.; Allen, W.P.; Williams, C.A.; Elsea, S.H. Haploinsufficiency of MBD5 associated with a syndrome involving microcephaly, intellectual disabilities, severe speech impairment, and seizures. *Eur. J. Hum. Genet.* **2010**, *18*, 436–441. [CrossRef] [PubMed]
38. Talkowski, M.E.; Mullegama, S.V.; Rosenfeld, J.A.; van Bon, B.W.; Shen, Y.; Repnikova, E.A.; Gastier-Foster, J.; Thrush, D.L.; Kathiresan, S.; Ruderfer, D.M.; et al. Assessment of 2q23.1 microdeletion syndrome implicates MBD5 as a single causal locus of intellectual disability, epilepsy, and autism spectrum disorder. *Am. J. Hum. Genet.* **2011**, *89*, 551–563. [CrossRef]
39. Amir, R.E.; Van den Veyver, I.B.; Wan, M.; Tran, C.Q.; Francke, U.; Zoghbi, H.Y. Rett syndrome is caused by mutations in X-linked MECP2, encoding methyl-CpG-binding protein 2. *Nat. Genet.* **1999**, *23*, 185–188. [CrossRef]
40. Lam, C.W.; Yeung, W.L.; Ko, C.H.; Poon, P.M.; Tong, S.F.; Chan, K.Y.; Lo, I.F.; Chan, L.Y.; Hui, J.; Wong, V.; et al. Spectrum of mutations in the MECP2 gene in patients with infantile autism and Rett syndrome. *J. Med. Genet.* **2000**, *37*, E41. [CrossRef]

41. Risheg, H.; Graham, J.M., Jr.; Clark, R.D.; Rogers, R.C.; Opitz, J.M.; Moeschler, J.B.; Peiffer, A.P.; May, M.; Joseph, S.M.; Jones, J.R.; et al. A recurrent mutation in MED12 leading to R961W causes Opitz-Kaveggia syndrome. *Nat. Genet.* **2007**, *39*, 451–453. [CrossRef] [PubMed]
42. Schwartz, C.E.; Tarpey, P.S.; Lubs, H.A.; Verloes, A.; May, M.M.; Risheg, H.; Friez, M.J.; Futreal, P.A.; Edkins, S.; Teague, J.; et al. The original Lujan syndrome family has a novel missense mutation (p.N1007S) in the MED12 gene. *J. Med. Genet.* **2007**, *44*, 472–477. [CrossRef] [PubMed]
43. Vulto-van Silfhout, A.T.; de Vries, B.B.; van Bon, B.W.; Hoischen, A.; Ruiterkamp-Versteeg, M.; Gilissen, C.; Gao, F.; van Zwam, M.; Harteveld, C.L.; van Essen, A.J.; et al. Mutations in MED12 cause X-linked Ohdo syndrome. *Am. J. Hum. Genet.* **2013**, *92*, 401–406. [CrossRef] [PubMed]
44. Kaufmann, R.; Straussberg, R.; Mandel, H.; Fattal-Valevski, A.; Ben-Zeev, B.; Naamati, A.; Shaag, A.; Zenvirt, S.; Konen, O.; Mimouni-Bloch, A.; et al. Infantile cerebral and cerebellar atrophy is associated with a mutation in the MED17 subunit of the transcription preinitiation mediator complex. *Am. J. Hum. Genet.* **2010**, *87*, 667–670. [CrossRef]
45. Hashimoto, S.; Boissel, S.; Zarhrate, M.; Rio, M.; Munnich, A.; Egly, J.M.; Colleaux, L. MED23 mutation links intellectual disability to dysregulation of immediate early gene expression. *Science* **2011**, *333*, 1161–1163. [CrossRef]
46. Leal, A.; Huehne, K.; Bauer, F.; Sticht, H.; Berger, P.; Suter, U.; Morera, B.; Del Valle, G.; Lupski, J.R.; Ekici, A.; et al. Identification of the variant Ala335Val of MED25 as responsible for CMT2B2: Molecular data, functional studies of the SH3 recognition motif and correlation between wild-type MED25 and PMP22 RNA levels in CMT1A animal models. *Neurogenetics* **2009**, *10*, 275–287. [CrossRef] [PubMed]
47. Basel-Vanagaite, L.; Smirin-Yosef, P.; Essakow, J.L.; Tzur, S.; Lagovsky, I.; Maya, I.; Pasmanik-Chor, M.; Yeheskel, A.; Konen, O.; Orenstein, N.; et al. Homozygous MED25 mutation implicated in eye-intellectual disability syndrome. *Hum. Genet.* **2015**, *134*, 577–587. [CrossRef]
48. Willemsen, M.H.; Valles, A.; Kirkels, L.A.; Mastebroek, M.; Olde Loohuis, N.; Kos, A.; Wissink-Lindhout, W.M.; de Brouwer, A.P.; Nillesen, W.M.; Pfundt, R.; et al. Chromosome 1p21.3 microdeletions comprising DPYD and MIR137 are associated with intellectual disability. *J. Med. Genet.* **2011**, *48*, 810–818. [CrossRef]
49. Pinto, D.; Delaby, E.; Merico, D.; Barbosa, M.; Merikangas, A.; Klei, L.; Thiruvahindrapuram, B.; Xu, X.; Ziman, R.; Wang, Z.; et al. Convergence of genes and cellular pathways dysregulated in autism spectrum disorders. *Am. J. Hum. Genet.* **2014**, *94*, 677–694. [CrossRef]
50. Kleefstra, T.; Kramer, J.M.; Neveling, K.; Willemsen, M.H.; Koemans, T.S.; Vissers, L.E.; Wissink-Lindhout, W.; Fenckova, M.; van den Akker, W.M.; Kasri, N.N.; et al. Disruption of an EHMT1-associated chromatin-modification module causes intellectual disability. *Am. J. Hum. Genet.* **2012**, *91*, 73–82. [CrossRef]
51. Chong, S.S.; Pack, S.D.; Roschke, A.V.; Tanigami, A.; Carrozzo, R.; Smith, A.C.; Dobyns, W.B.; Ledbetter, D.H. A revision of the lissencephaly and Miller-Dieker syndrome critical regions in chromosome 17p13.3. *Hum. Mol. Genet.* **1997**, *6*, 147–155. [CrossRef] [PubMed]
52. Sakamoto, M.; Ono, J.; Okada, S.; Masuno, M.; Nakamura, Y.; Kurahashi, H. Alteration of the LIS1 gene in Japanese patients with isolated lissencephaly sequence or Miller-Dieker syndrome. *Hum. Genet.* **1998**, *103*, 586–589. [CrossRef] [PubMed]
53. Lower, K.M.; Turner, G.; Kerr, B.A.; Mathews, K.D.; Shaw, M.A.; Gedeon, A.K.; Schelley, S.; Hoyme, H.E.; White, S.M.; Delatycki, M.B.; et al. Mutations in PHF6 are associated with Borjeson-Forssman-Lehmann syndrome. *Nat. Genet.* **2002**, *32*, 661–665. [CrossRef]
54. Laumonnier, F.; Holbert, S.; Ronce, N.; Faravelli, F.; Lenzner, S.; Schwartz, C.E.; Lespinasse, J.; Van Esch, H.; Lacombe, D.; Goizet, C.; et al. Mutations in PHF8 are associated with X linked mental retardation and cleft lip/cleft palate. *J. Med. Genet.* **2005**, *42*, 780–786. [CrossRef]
55. de Brouwer, A.P.; Williams, K.L.; Duley, J.A.; van Kuilenburg, A.B.; Nabuurs, S.B.; Egmont-Petersen, M.; Lugtenberg, D.; Zoetekouw, L.; Banning, M.J.; Roeffen, M.; et al. Arts syndrome is caused by loss-of-function mutations in PRPS1. *Am. J. Hum. Genet.* **2007**, *81*, 507–518. [CrossRef] [PubMed]
56. Kim, H.J.; Sohn, K.M.; Shy, M.E.; Krajewski, K.M.; Hwang, M.; Park, J.H.; Jang, S.Y.; Won, H.H.; Choi, B.O.; Hong, S.H.; et al. Mutations in PRPS1, which encodes the phosphoribosyl pyrophosphate synthetase enzyme critical for nucleotide biosynthesis, cause hereditary peripheral neuropathy with hearing loss and optic neuropathy (cmtx5). *Am. J. Hum. Genet.* **2007**, *81*, 552–558. [CrossRef]
57. Liu, X.; Han, D.; Li, J.; Han, B.; Ouyang, X.; Cheng, J.; Li, X.; Jin, Z.; Wang, Y.; Bitner-Glindzicz, M.; et al. Loss-of-function mutations in the PRPS1 gene cause a type of nonsyndromic X-linked sensorineural deafness, DFN2. *Am. J. Hum. Genet.* **2010**, *86*, 65–71. [CrossRef]
58. Noor, A.; Whibley, A.; Marshall, C.R.; Gianakopoulos, P.J.; Piton, A.; Carson, A.R.; Orlic-Milacic, M.; Lionel, A.C.; Sato, D.; Pinto, D.; et al. Disruption at the PTCHD1 Locus on Xp22.11 in Autism spectrum disorder and intellectual disability. *Sci. Transl. Med.* **2010**, *2*, 49ra68. [CrossRef]
59. Chaudhry, A.; Noor, A.; Degagne, B.; Baker, K.; Bok, L.A.; Brady, A.F.; Chitayat, D.; Chung, B.H.; Cytrynbaum, C.; Dyment, D.; et al. Phenotypic spectrum associated with PTCHD1 deletions and truncating mutations includes intellectual disability and autism spectrum disorder. *Clin. Genet.* **2015**, *88*, 224–233. [CrossRef]

60. Tatour, Y.; Sanchez-Navarro, I.; Chervinsky, E.; Hakonarson, H.; Gawi, H.; Tahsin-Swafiri, S.; Leibu, R.; Lopez-Molina, M.I.; Fernandez-Sanz, G.; Ayuso, C.; et al. Mutations in SCAPER cause autosomal recessive retinitis pigmentosa with intellectual disability. *J. Med. Genet.* **2017**, *54*, 698–704. [CrossRef]
61. Hoischen, A.; van Bon, B.W.; Gilissen, C.; Arts, P.; van Lier, B.; Steehouwer, M.; de Vries, P.; de Reuver, R.; Wieskamp, N.; Mortier, G.; et al. De novo mutations of SETBP1 cause Schinzel-Giedion syndrome. *Nat. Genet.* **2010**, *42*, 483–485. [CrossRef] [PubMed]
62. Filges, I.; Shimojima, K.; Okamoto, N.; Rothlisberger, B.; Weber, P.; Huber, A.R.; Nishizawa, T.; Datta, A.N.; Miny, P.; Yamamoto, T. Reduced expression by SETBP1 haploinsufficiency causes developmental and expressive language delay indicating a phenotype distinct from Schinzel-Giedion syndrome. *J. Med. Genet.* **2011**, *48*, 117–122. [CrossRef] [PubMed]
63. Marseglia, G.; Scordo, M.R.; Pescucci, C.; Nannetti, G.; Biagini, E.; Scandurra, V.; Gerundino, F.; Magi, A.; Benelli, M.; Torricelli, F. 372 kb microdeletion in 18q12.3 causing SETBP1 haploinsufficiency associated with mild mental retardation and expressive speech impairment. *Eur. J. Med. Genet.* **2012**, *55*, 216–221. [CrossRef]
64. Hellman-Aharony, S.; Smirin-Yosef, P.; Halevy, A.; Pasmanik-Chor, M.; Yeheskel, A.; Har-Zahav, A.; Maya, I.; Straussberg, R.; Dahary, D.; Haviv, A.; et al. Microcephaly thin corpus callosum intellectual disability syndrome caused by mutated TAF2. *Pediatr. Neurol.* **2013**, *49*, 411–416.e411. [CrossRef] [PubMed]
65. Langouet, M.; Saadi, A.; Rieunier, G.; Moutton, S.; Siquier-Pernet, K.; Fernet, M.; Nitschke, P.; Munnich, A.; Stern, M.H.; Chaouch, M.; et al. Mutation in TTI2 reveals a role for triple T complex in human brain development. *Hum. Mutat.* **2013**, *34*, 1472–1476. [CrossRef]
66. Tischfield, M.A.; Baris, H.N.; Wu, C.; Rudolph, G.; Van Maldergem, L.; He, W.; Chan, W.M.; Andrews, C.; Demer, J.L.; Robertson, R.L.; et al. Human TUBB3 mutations perturb microtubule dynamics, kinesin interactions, and axon guidance. *Cell* **2010**, *140*, 74–87. [CrossRef]
67. Poirier, K.; Saillour, Y.; Bahi-Buisson, N.; Jaglin, X.H.; Fallet-Bianco, C.; Nabbout, R.; Castelnau-Ptakhine, L.; Roubertie, A.; Attie-Bitach, T.; Desguerre, I.; et al. Mutations in the neuronal ss-tubulin subunit TUBB3 result in malformation of cortical development and neuronal migration defects. *Hum. Mol. Genet.* **2010**, *19*, 4462–4473. [CrossRef]
68. Bilguvar, K.; Ozturk, A.K.; Louvi, A.; Kwan, K.Y.; Choi, M.; Tatli, B.; Yalnizoglu, D.; Tuysuz, B.; Caglayan, A.O.; Gokben, S.; et al. Whole-exome sequencing identifies recessive WDR62 mutations in severe brain malformations. *Nature* **2010**, *467*, 207–210. [CrossRef]
69. Nicholas, A.K.; Khurshid, M.; Desir, J.; Carvalho, O.P.; Cox, J.J.; Thornton, G.; Kausar, R.; Ansar, M.; Ahmad, W.; Verloes, A.; et al. WDR62 is associated with the spindle pole and is mutated in human microcephaly. *Nat. Genet.* **2010**, *42*, 1010–1014. [CrossRef]
70. Hirata, H.; Nanda, I.; van Riesen, A.; McMichael, G.; Hu, H.; Hambrock, M.; Papon, M.A.; Fischer, U.; Marouillat, S.; Ding, C.; et al. ZC4H2 mutations are associated with arthrogryposis multiplex congenita and intellectual disability through impairment of central and peripheral synaptic plasticity. *Am. J. Hum. Genet.* **2013**, *92*, 681–695. [CrossRef]
71. Frints, S.G.M.; Hennig, F.; Colombo, R.; Jacquemont, S.; Terhal, P.; Zimmerman, H.H.; Hunt, D.; Mendelsohn, B.A.; Kordass, U.; Webster, R.; et al. Deleterious de novo variants of X-linked ZC4H2 in females cause a variable phenotype with neurogenic arthrogryposis multiplex congenita. *Hum. Mutat.* **2019**, *40*, 2270–2285. [CrossRef] [PubMed]
72. Balemans, M.C.; Kasri, N.N.; Kopanitsa, M.V.; Afinowi, N.O.; Ramakers, G.; Peters, T.A.; Beynon, A.J.; Janssen, S.M.; van Summeren, R.C.; Eeftens, J.M.; et al. Hippocampal dysfunction in the Euchromatin histone methyltransferase 1 heterozygous knockout mouse model for Kleefstra syndrome. *Hum. Mol. Genet.* **2013**, *22*, 852–866. [CrossRef] [PubMed]
73. Tachibana, M.; Ueda, J.; Fukuda, M.; Takeda, N.; Ohta, T.; Iwanari, H.; Sakihama, T.; Kodama, T.; Hamakubo, T.; Shinkai, Y. Histone methyltransferases G9a and GLP form heteromeric complexes and are both crucial for methylation of euchromatin at H3-K9. *Genes Dev.* **2005**, *19*, 815–826. [CrossRef] [PubMed]
74. Gambino, F.; Kneib, M.; Pavlowsky, A.; Skala, H.; Heitz, S.; Vitale, N.; Poulain, B.; Khelfaoui, M.; Chelly, J.; Billuart, P.; et al. IL1RAPL1 controls inhibitory networks during cerebellar development in mice. *Eur. J. Neurosci.* **2009**, *30*, 1476–1486. [CrossRef] [PubMed]
75. Shahbazian, M.; Young, J.; Yuva-Paylor, L.; Spencer, C.; Antalffy, B.; Noebels, J.; Armstrong, D.; Paylor, R.; Zoghbi, H. Mice with truncated MeCP2 recapitulate many Rett syndrome features and display hyperacetylation of histone H3. *Neuron* **2002**, *35*, 243–254. [CrossRef] [PubMed]
76. Iacono, G.; Dubos, A.; Meziane, H.; Benevento, M.; Habibi, E.; Mandoli, A.; Riet, F.; Selloum, M.; Feil, R.; Zhou, H.; et al. Increased H3K9 methylation and impaired expression of Protocadherins are associated with the cognitive dysfunctions of the Kleefstra syndrome. *Nucleic Acids Res.* **2018**, *46*, 4950–4965. [CrossRef]
77. Nagano, T.; Mitchell, J.A.; Sanz, L.A.; Pauler, F.M.; Ferguson-Smith, A.C.; Feil, R.; Fraser, P. The Air noncoding RNA epigenetically silences transcription by targeting G9a to chromatin. *Science* **2008**, *322*, 1717–1720. [CrossRef]
78. Mantamadiotis, T.; Lemberger, T.; Bleckmann, S.C.; Kern, H.; Kretz, O.; Martin Villalba, A.; Tronche, F.; Kellendonk, C.; Gau, D.; Kapfhammer, J.; et al. Disruption of CREB function in brain leads to neurodegeneration. *Nat. Genet.* **2002**, *31*, 47–54. [CrossRef]
79. Monory, K.; Massa, F.; Egertova, M.; Eder, M.; Blaudzun, H.; Westenbroek, R.; Kelsch, W.; Jacob, W.; Marsch, R.; Ekker, M.; et al. The endocannabinoid system controls key epileptogenic circuits in the hippocampus. *Neuron* **2006**, *51*, 455–466. [CrossRef]
80. Hill, R.A.; Natsume, R.; Sakimura, K.; Nishiyama, A. NG2 cells are uniformly distributed and NG2 is not required for barrel formation in the somatosensory cortex. *Mol. Cell Neurosci.* **2011**, *46*, 689–698. [CrossRef]
81. Dickinson, M.E.; Flenniken, A.M.; Ji, X.; Teboul, L.; Wong, M.D.; White, J.K.; Meehan, T.F.; Weninger, W.J.; Westerberg, H.; Adissu, H.; et al. High-throughput discovery of novel developmental phenotypes. *Nature* **2016**, *537*, 508–514. [CrossRef] [PubMed]

82. Karp, N.A.; Meehan, T.F.; Morgan, H.; Mason, J.C.; Blake, A.; Kurbatova, N.; Smedley, D.; Jacobsen, J.; Mott, R.F.; Iyer, V.; et al. Applying the ARRIVE Guidelines to an In Vivo Database. *PLoS Biol.* **2015**, *13*, e1002151. [CrossRef]
83. Riet, F.; Mittelhaeuser, C.; Lux, A.; Bour, R.; Selloum, M.; Sorg, T.; Herault, Y.; Meziane, H. Behavioral Testing Design for Evaluation of Cognitive Disabilities. *Curr. Protoc.* **2022**, *2*, e382. [CrossRef] [PubMed]
84. Cacheiro, P.; Munoz-Fuentes, V.; Murray, S.A.; Dickinson, M.E.; Bucan, M.; Nutter, L.M.J.; Peterson, K.A.; Haselimashhadi, H.; Flenniken, A.M.; Morgan, H.; et al. Human and mouse essentiality screens as a resource for disease gene discovery. *Nat. Commun.* **2020**, *11*, 655. [CrossRef]
85. Dubos, A.; Castells-Nobau, A.; Meziane, H.; Oortveld, M.A.; Houbaert, X.; Iacono, G.; Martin, C.; Mittelhaeuser, C.; Lalanne, V.; Kramer, J.M.; et al. Conditional depletion of intellectual disability and Parkinsonism candidate gene ATP6AP2 in fly and mouse induces cognitive impairment and neurodegeneration. *Hum. Mol. Genet.* **2015**, *24*, 6736–6755. [CrossRef] [PubMed]
86. Ung, D.C.; Iacono, G.; Meziane, H.; Blanchard, E.; Papon, M.A.; Selten, M.; van Rhijn, J.R.; Montjean, R.; Rucci, J.; Martin, S.; et al. Ptchd1 deficiency induces excitatory synaptic and cognitive dysfunctions in mouse. *Mol. Psychiatry* **2018**, *23*, 1356–1367. [CrossRef] [PubMed]
87. Schinzel, A.; Giedion, A. A syndrome of severe midface retraction, multiple skull anomalies, clubfeet, and cardiac and renal malformations in sibs. *Am. J. Med. Genet.* **1978**, *1*, 361–375. [CrossRef]
88. Jansen, N.A.; Braden, R.O.; Srivastava, S.; Otness, E.F.; Lesca, G.; Rossi, M.; Nizon, M.; Bernier, R.A.; Quelin, C.; van Haeringen, A.; et al. Clinical delineation of SETBP1 haploinsufficiency disorder. *Eur. J. Hum. Genet.* **2021**, *29*, 1198–1205. [CrossRef]
89. Tischfield, M.A.; Cederquist, G.Y.; Gupta, M.L., Jr.; Engle, E.C. Phenotypic spectrum of the tubulin-related disorders and functional implications of disease-causing mutations. *Curr. Opin Genet. Dev.* **2011**, *21*, 286–294. [CrossRef] [PubMed]
90. Stewart, D.R.; Kleefstra, T. The chromosome 9q subtelomere deletion syndrome. *Am. J. Med. Genet. Part C Semin. Med. Genet.* **2007**, *145C*, 383–392. [CrossRef]
91. Balemans, M.C.; Huibers, M.M.; Eikelenboom, N.W.; Kuipers, A.J.; van Summeren, R.C.; Pijpers, M.M.; Tachibana, M.; Shinkai, Y.; van Bokhoven, H.; Van der Zee, C.E. Reduced exploration, increased anxiety, and altered social behavior: Autistic-like features of euchromatin histone methyltransferase 1 heterozygous knockout mice. *Behav. Brain Res.* **2010**, *208*, 47–55. [CrossRef] [PubMed]
92. Schaefer, A.; Sampath, S.C.; Intrator, A.; Min, A.; Gertler, T.S.; Surmeier, D.J.; Tarakhovsky, A.; Greengard, P. Control of cognition and adaptive behavior by the GLP/G9a epigenetic suppressor complex. *Neuron* **2009**, *64*, 678–691. [CrossRef] [PubMed]
93. Shoubridge, C.; Fullston, T.; Gecz, J. ARX spectrum disorders: Making inroads into the molecular pathology. *Hum. Mutat.* **2010**, *31*, 889–900. [CrossRef] [PubMed]
94. Tekin, M.; Kavaz, A.; Berberoglu, M.; Fitoz, S.; Ekim, M.; Ocal, G.; Akar, N. The KBG syndrome: Confirmation of autosomal dominant inheritance and further delineation of the phenotype. *Am. J. Med. Genet. Part A* **2004**, *130A*, 284–287. [CrossRef]
95. Gupta, H.V.; Vengoechea, J.; Sahaya, K.; Virmani, T. A splice site mutation in ATP6AP2 causes X-linked intellectual disability, epilepsy, and parkinsonism. *Park. Relat. Disord.* **2015**, *21*, 1473–1475. [CrossRef] [PubMed]
96. Synofzik, M.; Muller vom Hagen, J.; Haack, T.B.; Wilhelm, C.; Lindig, T.; Beck-Wodl, S.; Nabuurs, S.B.; van Kuilenburg, A.B.; de Brouwer, A.P.; Schols, L. X-linked Charcot-Marie-Tooth disease, Arts syndrome, and prelingual non-syndromic deafness form a disease continuum: Evidence from a family with a novel PRPS1 mutation. *Orphanet J. Rare Dis.* **2014**, *9*, 24. [CrossRef]
97. Roessler, B.J.; Nosal, J.M.; Smith, P.R.; Heidler, S.A.; Palella, T.D.; Switzer, R.L.; Becker, M.A. Human X-linked phosphoribosylpyrophosphate synthetase superactivity is associated with distinct point mutations in the PRPS1 gene. *J. Biol. Chem.* **1993**, *268*, 26476–26481. [CrossRef]
98. Becker, M.A.; Smith, P.R.; Taylor, W.; Mustafi, R.; Switzer, R.L. The genetic and functional basis of purine nucleotide feedback-resistant phosphoribosylpyrophosphate synthetase superactivity. *J. Clin. Investig.* **1995**, *96*, 2133–2141. [CrossRef]
99. Brancati, F.; D'Avanzo, M.G.; Digilio, M.C.; Sarkozy, A.; Biondi, M.; De Brasi, D.; Mingarelli, R.; Dallapiccola, B. KBG syndrome in a cohort of Italian patients. *Am. J. Med. Genet. A* **2004**, *131*, 144–149. [CrossRef]
100. Bowl, M.R.; Simon, M.M.; Ingham, N.J.; Greenaway, S.; Santos, L.; Cater, H.; Taylor, S.; Mason, J.; Kurbatova, N.; Pearson, S.; et al. A large scale hearing loss screen reveals an extensive unexplored genetic landscape for auditory dysfunction. *Nat. Commun.* **2017**, *8*, 886. [CrossRef]